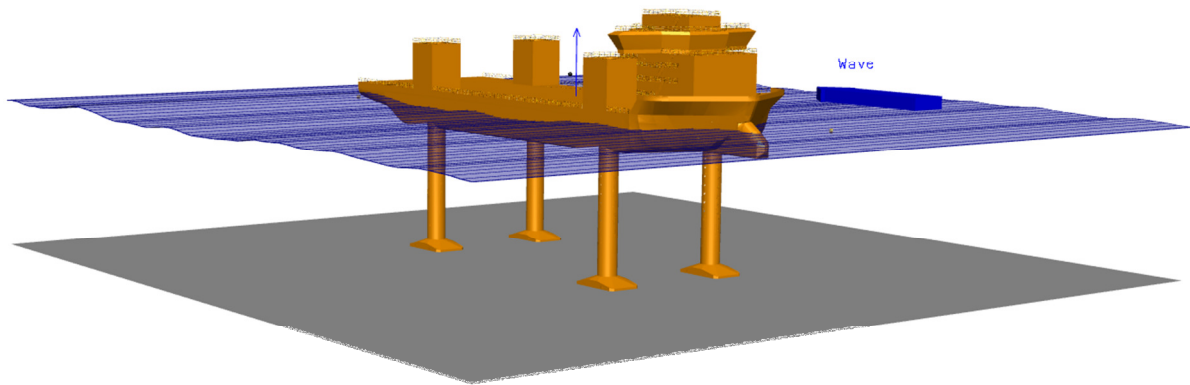


CHALMERS



Impact loads on a self-elevating unit during jacking operation

A methodology incorporating site-specific parameters for
weather window assessment

*Master's Thesis in the International Master's Programme Naval Architecture and
Ocean Engineering*

VIKTOR DAUN AND FREDRIK OLSSON

Department of Shipping and Marine Technology
Division of Marine Design, Research Group Marine Structures
CHALMERS UNIVERSITY OF TECHNOLOGY
Göteborg, Sweden 2014
Master's thesis 2014:X-14/299

MASTER'S THESIS IN THE INTERNATIONAL MASTER'S PROGRAMME IN
NAVAL ARCHITECTURE AND OCEAN ENGINEERING

Impact loads on a self-elevating unit during jacking operation

A methodology incorporating site-specific parameters for weather window assessment

VIKTOR DAUN AND FREDRIK OLSSON

Department of Shipping and Marine Technology
Division of Marine Design
Research Group Marine Structures
CHALMERS UNIVERSITY OF TECHNOLOGY
Göteborg, Sweden 2014

Impact loads on a self-elevating unit during jacking operation
A methodology incorporating site-specific parameters for weather window assessment
VIKTOR DAUN AND FREDRIK OLSSON

© VIKTOR DAUN AND FREDRIK OLSSON 2014

Master's Thesis 2014:X-14/299
Department of Shipping and Marine Technology
Division of Marine Design
Research Group Marine Structures
Chalmers University of Technology
SE-412 96 Göteborg
Sweden
Telephone: + 46 (0)31-772 1000

Cover:
Calculation domain in SIMO for time-domain simulations. External hull geometry file is used. Courtesy of Fred. Olsen Windcarrier AS.

Printed by Chalmers Reproservice
Göteborg, Sweden 2014

MASTER'S THESIS IN THE INTERNATIONAL MASTER'S PROGRAMME IN
NAVAL ARCHITECTURE AND OCEAN ENGINEERING

Impact loads on a self-elevating unit during jacking operation
A methodology incorporating site-specific parameters for weather window assessment

VIKTOR DAUN AND FREDRIK OLSSON

Department of Shipping and Marine Technology
Division of Marine Design
Research Group Marine Structures
CHALMERS UNIVERSITY OF TECHNOLOGY
Göteborg, Sweden 2014

Impact loads on a self-elevating unit during jacking operation
A methodology incorporating site-specific parameters for weather window assessment
Master's Thesis in the International Master's Programme in Naval Architecture and
Ocean Engineering

VIKTOR DAUN AND FREDRIK OLSSON

Department of Shipping and Marine Technology
Division of Marine Design, Research Group Marine Structures
Chalmers University of Technology

ABSTRACT

The renewable energy resource of offshore wind is believed to have a great potential in playing an essential role on the future energy market in Europe, but there are complications such as harsh weather and low accessibility. To manage this, most offshore wind turbines of today are installed and maintained using self-elevating units (SEUs). Even though SEUs provide stable platforms easing offshore operations once in an elevated mode, the installation and retrieval phases of the unit itself remain a limiting factor for operation, as impact between the seabed and spudcan may occur due to vessel motion in waves. Limits for these operations are defined by the vessel manufacturer and do generally not account for site-specific parameters, such as soil deformation behaviour and water depth. Neither does the recommended practice for estimating impact loads by classification societies.

The objective of this thesis is to develop a method of analysis by which it will be possible to make weather window assessments for the installation and retrieval phases of a SEU. The method of analysis takes site-specific parameters, defined as soil type and water depth, into account in addition to vessel-specific and environmental parameters. The inclusion of site-specific parameters is the novel contribution compared to assessment methodologies used today.

A simulation model is developed incorporating a coupled non-linear time-domain analysis of vessel motion and soil-structure interaction. Soil deformation behaviour during impact is described by resistance curves based on a bearing capacity theory, an existing theory initially used for in-situ testing of soils. In addition to the time-domain simulation, an un-coupled FE analysis of structural capacity is made. A structural evaluation criterion against which impact forces are compared is used for weather window assessments. The simulation model is applied on a case study utilizing different soil types to study impact forces and the capacity of the structure for withstanding such impacts and eventually performing a weather window assessment.

It has been found that the jacking operation can be divided into two different phases when it comes to loads on the spudcan. A first phase is dominated by vertical forces, which is the focus in this thesis, followed by a phase dominated by horizontal forces. Results from the case study show that including soil deformation behaviour is of paramount importance to the magnitude of the resulting impact forces and that class-recommended practice does indeed produce rather large force estimates. Thus, assessments where site-specific parameters are incorporated could definitely increase the operable weather window for SEUs, and, consequently, increase the economic competitiveness of, for example, the offshore wind industry.

Keywords: self-elevating unit, installation, retrieval, impact loads, limiting seastate, structural capacity, weather window, bearing capacity.

Stötkrafter på jack-up fartyg under installationsproceduren

En metodik som inkluderar platsspecifika parametrar för utvärdering av väderfönster

Examensarbete inom Naval Architecture and Ocean Engineering

VIKTOR DAUN AND FREDRIK OLSSON

Institutionen för sjöfart och marin teknik

Avdelningen för Marine Design

Forskargruppen Marine Structures

Chalmers tekniska högskola

SAMMANFATTNING

Den förnybara energikällan havsbaserad vindkraft tros ha stor potential och spela en viktig roll på den framtida energimarknaden men komplikationer såsom hårt väder och låg tillgänglighet försvårar. För att hantera detta är de flesta havsbaserade vindkraftverk idag installerade och underhållna med jack-up fartyg. Även om jack-up fartyg är stabila plattformar i upplyft läge förblir installationsfasen av fartyget självt en begränsande faktor då stötar mellan havsbotten och foten kan uppstå som en följd av fartygets rörelser i vågor. Begränsande sjöförhållanden för dessa operationer definieras av designern och tar i allmänhet inte hänsyn till platsspecifika parametrar såsom deformation av havsbotten eller vattendjup. Inte heller den av klassningssällskap rekommenderade praxisen för uppskattning av stötkrafter tar hänsyn till dessa parametrar.

Syftet med detta examensarbete är att utveckla en analysmetodik med vars hjälp utvärderingar av väderfönstret för installation och avinstallationsfaserna för ett jack-up fartyg. Analysmetodiken skall ta hänsyn till platsspecifika parametrar såsom botten typ och vattendjup i tillägg till fartygsspecifika och miljöspecifika parametrar. Inkluderandet av platsspecifika parametrar är det nya bidraget i jämförelse med existerande analysmetodiker använda idag.

En simuleringsmodell har utvecklats, innehållandes en kopplad olinjär tidsdomänanalys av fartygsrörelser och interaktionen mellan havsbotten och struktur. Havsbottens deformationsbeteende under stöten beskrivs av motståndskurvor baserade på bärighetsteori, en existerande teori som ursprungligen utvecklades för in-situ testning av jordar. Därtill görs okopplade FE analyser av den strukturella kapaciteten. Ett strukturellt kriterium för utvärdering av väderfönstret används gentemot vilket stötkrafterna jämförs. Simuleringsmodellen tillämpas på en fallstudie som använder olika jordtyper för att studera stötkrafterna och förmågan hos strukturen för att motstå sådana krafter. Slutligen görs en bedömning av väderfönstret.

Simuleringar visar att jackingoperationen kan delas in i två olika faser med avseende på belastningar på foten. En första fas som domineras av vertikala krafter, fokus i denna avhandling, följt av en fas som domineras av horisontella krafter. Resultaten från fallstudien visar att effekten av att inkludera havsbottens deformationsbeteende är av största vikt för de resulterande stötkrafternas magnitud och att den av klass rekommenderade praxisen producerar förhållandevis stora uppskattningar av stötkrafter. Bedömningar där platsspecifika parametrar ingår kan således definitivt öka väderfönster för jack-up fartyg och därmed öka den ekonomiska konkurrenskraften i exempelvis industrin runt havsbaserad vindkraft.

Nyckelord: begränsande sjöförhållanden, bärighetsteori, installation, jack-up fartyg, strukturell kapacitet, stötkrafter, väderfönster.

Contents

1	INTRODUCTION	1
1.1	Self-elevating units	1
1.2	Objective	3
1.3	Methodology	4
1.4	Limitations	6
1.5	Outline of thesis	7
2	IMPACT MECHANICS	9
2.1	Classical mechanics approach	10
2.2	Contact mechanics approach	10
2.3	Impact in soil	11
2.3.1	Soil mechanics	11
2.3.2	Cone penetration test	12
2.4	Concluding remarks	13
2.5	Bearing capacity theory	14
2.5.1	Penetration in clay	14
2.5.2	Penetration in silica sands	15
2.5.3	Load rate effects on soil deformation behavior	15
3	SIMULATION MODEL	17
3.1	Hydrodynamic submodel	19
3.2	Impact submodel	20
3.2.1	The SIMO soil penetration feature	20
3.3	Structural submodel	21
3.3.1	Mesh	22
4	MODEL VERIFICATION	25
4.1	Hydrodynamic model	25
4.2	FE model	25
4.3	Geotechnical verification	26
4.3.1	Vertical capacity	26
4.3.2	Horizontal capacity	28
5	CASE STUDY	31
5.1	Time-domain simulation procedure	31
5.2	FE simulation procedure	32
5.2.1	Structural evaluation criteria	33
5.2.2	Loads and boundary conditions	34

6	RESULTS	37
6.1	Impact forces	37
6.2	Structural capacity	40
6.3	Weather window	44
7	DISCUSSION	47
8	CONCLUSIONS	51
9	FUTURE WORK	53
10	REFERENCES	55
	APPENDIX A HYDRODYNAMIC MODEL	
	APPENDIX B GEOTECHNICAL MODEL	
	APPENDIX C FE SIMULATION RESULTS	

Preface

This thesis is a part of the requirements for the master's degree in Naval Architecture and Ocean Engineering at Chalmers University of Technology, Göteborg, and has been carried out partly at the division for Offshore wind at Statoil ASA, Trondheim, and partly at the Division of Marine Design, Department of Shipping and Marine Technology, Chalmers University of Technology between January and June of 2014.

We would like to acknowledge and thank our examiner and supervisor, Professor Jonas Ringsberg at the Department of Shipping and Marine Technology, for his excellent guidance and support throughout the work with this thesis. We would also like to thank Rune Yttervik, our supervisor at Statoil ASA, for his valuable time and professional guidance and support. Furthermore, we would like to thank Geir Svanø at Statoil ASA for his assistance within geotechnical matters.

Finally, we would like to thank Fred. Olsen Windcarrier for taking an interest in the topic of our master's thesis and for being very supportive in supplying necessary data. Special thanks to Petter Faye Søyland and Håkon Halseth Johannesen. Most of this data is, however, subject to confidentiality and cannot be presented in the thesis. For inquiries on the matter, please contact the authors.

Göteborg, May 2014

Viktor Daun and Fredrik Olsson

Abbreviations

DNV	Det Norske Veritas
DOF	Degree of Freedom
DP	Dynamic Positioning
EC	European Commission
FE	Finite Element
ISO	International Organization for Standardization
RAO	Response Amplitude Operator
SEU	Self-Elevating Unit
SNAME	The Society of Naval Architects and Marine Engineers
UF	Usage Factor

Notations

Roman upper case letters

A	Equivalent contact area [m ²]
A _{steel}	Nominal cross-sectional area of structural member [m ²]
B	Diameter of equivalent contact area [m]
D	Diameter [m]
D _p	Penetration depth [m]
C _D	Drag coefficient [-]
C _M	Inertia coefficient [-]
F _{cr}	Critical force defining failure [N]
I _m	Mass moment of inertia of the unit [kgm ²]
K _t	Stress concentration factor [-]
L	Length [m]
M	Bending moment [Nm]
R	Radius [m]
T	Period of motion [s]

Roman lower case letters

c	Damping coefficient [Ns/m]
d	Horizontal distance between a leg and the center of flotation [m]
h	Water depth [m]
k	Stiffness coefficient [N/m]

k_H	Overall lateral stiffness of a leg [N/m]
k_V	Overall vertical stiffness of a leg [N/m]
m	Mass of body [kg]
m_a	Added mass/hydrodynamic mass [kg]
t	Time variable [s]
r	Radius [m]
x	Position [m]
\dot{x}	Velocity [m/s]
\ddot{x}	Acceleration [m/s ²]

Greek upper case letters

θ	Amplitude of motion [rad]
----------	---------------------------

Greek lower case letters

γ'	Submerged unit weight of soil [N/m ³]
λ	Slenderness [-]
μ	Soil shear modulus [Pa]
ν	Poisson ratio [-]
ρ	Density [kg/m ³]
σ_{cr}	Critical compensated buckling stress [Pa]
σ_E	Critical elastic buckling stress [Pa]
σ_{XX}	Stress in the XX-direction [Pa]
σ_y	Yield stress [Pa]
ϕ	Friction angle [degrees]

1 Introduction

In order to reach a sustainable way of meeting the world's demand for energy and transportation, our society needs to phase out the dependency of fossil fuel that is and has been present during the major part of the last century. The importance of renewable energy sources such as sun, wind and waves and the utilization of these are increasingly growing (R.E.H. Sims et al., 2007). Offshore wind is a renewable energy resource that will play an essential role on the future energy market in Europe. The European Commission (2008) states that offshore wind has several key advantages compared to land-based wind power. Firstly, larger turbines are feasible at offshore locations. The size of land-based turbines are restricted by transportation difficulties. Secondly, the utilization rate increases when wind turbines move offshore since wind resources are larger and more stable. Thirdly, noise and vibrations produced by the turbines are kept well away from populated areas, decreasing the risk of concerns raised about this. However, the environment is harsher offshore than onshore and accessibility is lower for apparent reasons. Installation and maintenance are complicated marine operations (EC, 2008). Facing challenges linked to installation and maintenance, it is possible to use proven technology from the offshore oil and gas industry. Different kinds of platforms for drilling and production have been used for many years in the offshore oil and gas industry and self-elevating units are nowadays also often used for installing various components of offshore wind turbines on locations with a moderate water depth (DNV, 2013), see Figure 1.1.

1.1 Self-elevating units

A self-elevating unit (SEU), sometimes called a jack-up rig, jack-up vessel or self-elevating vessel is a floating platform equipped with legs, typically three or four, with which the vessel can extract to the bottom and lift itself up upon in order to get the hull away from the wave zone. The legs are usually separated and fitted with special footings (spudcans) designed for penetration of the seabed. Some SEUs are fitted with legs that are connected to a large mat to prevent extreme penetration into the seabed. The legs are often lattice structures of a triangular or square cross-section or tubulars of circular or square cross-sections. Spudcans are large, often cylindrical or almost cylindrical structures usually with a conical base. Fitted to the lower end of the legs on a SEU, they support the structure when in an elevated position (DNV, 2012). In cases where the legs are of a tubular cross-section they can have spudcans attached in the bottom, but there are also cases where the cross-section is closed and the leg itself penetrates the seabed. SEUs are used for marine operations offshore and the operational modes are identified as (ISO, 2012):

- Transit, in which the SEU moves from one location to another, either by itself or by tug boats, with the legs retracted.
- Installation, in which the SEU installs itself by positioning its legs on the seabed and raising the hull safely away from the wave zone. A preloading procedure, to assure sufficient bearing capacity of the seabed, is also conducted during this phase.
- Operation, in which the SEU is fixed on location in an elevated position with its hull above the wave zone and capable of other tasks such as exploration drilling, wind turbine installation, etc. See Figure 1.1.
- Retrieval, in which the SEU retracts its legs from the seabed and becomes ready to move to a new location.



Figure 1.1 The Gusto MSC NG9000C-HPE in elevated mode installing a pre-assembled rotor on a bottom-fixed offshore wind turbine. (Courtesy of Fred. Olsen Windcarrier AS).

All locations being the objective of a jack-up operation should be assessed to evaluate suitability and possible risks. However, if a new location has parameters equal to a previous location these can be used in the assessment (SNAME, 2008). To perform a location assessment certain data is to be collected:

- Rig data. The rig type including drawings, specifications, weights, material, preloading capability, etc., is needed to assess the suitability for the location. Structural details such as leg, spudcan and jackhouse should also be considered by a suitable model to account for flexibility and stiffnesses in the structure.
- Geotechnical data. In order to evaluate the bearing force of the seabed it is important to know the geotechnical conditions on the site. This data could be described by seismic data, coring data, cone-penetrometer data or other geotechnical surveys. The needed amount of data varies depending on the kind of soil and the type of jack-up. An evaluation of shallow gas deposits and previous jack-up footprints should also be performed (SNAME, 2008).
- Environmental data. The environmental parameters needed are wind, waves and current. For wind and waves it is recommended to use the 50 year return extremes. In some cases it can be valid to use other return periods depending on whether the vessel is manned or on the risk of marine pollution. In some cases it could also be necessary to include tides, ice, earthquakes, rate of marine growth, etc., in the assessment.
- Site data. The location coordinates, seabed topography and water depths (for different tides if necessary) is needed to assess the location.

These data are used for evaluating the structural integrity, foundational bearing force and overturning stability of the vessel in operation mode at the specific location (SNAME, 2008). When the SEU arrives at the location for the intended operation it positions itself using tug boats or a dynamic positioning (DP) system. SEUs used in the offshore wind industry are mostly self-propelled. The legs are lowered using a mechanic or hydraulic system in the jackhouse until the spudcans reach the seabed and make initial contact with the seabed. Preloading of the legs is performed to ensure sufficient foundation capacity, and elevation of the hull is continued until a pre-specified airgap is reached.

1.2 Objective

The installation and retrieval phases of a SEU are two of the key operating limiting factors, and the phases when the legs are being set down onto and lifted up from the seabed are particularly critical as impacts may occur due to vessel motion in waves (DNV, 2013), see Figure 1.2. The operable limit for these operation modes is today decided by the manufacturer of the particular vessel. The ship owner is provided with a table of limiting seastates which the vessel should be operated by. In this thesis, such an interval in the H_s/T_p -domain in which a vessel is allowed to operate is referred to as weather window. The weather window, as provided by the manufacturer, is made up of general criteria calculated by worst case assumptions, accounting for vessel-specific parameters such as hull geometry and structural arrangement and environmental parameters such as seastate and wave heading. Site-specific parameters such as soil type and water depth are not accounted for. In addition, class recommended practice (DNV, 2012) regarding the installation of SEUs is believed to produce large estimates of impact forces, as extensive simplifications are made in the recommended calculation procedures and site-specific parameters are not accounted for.

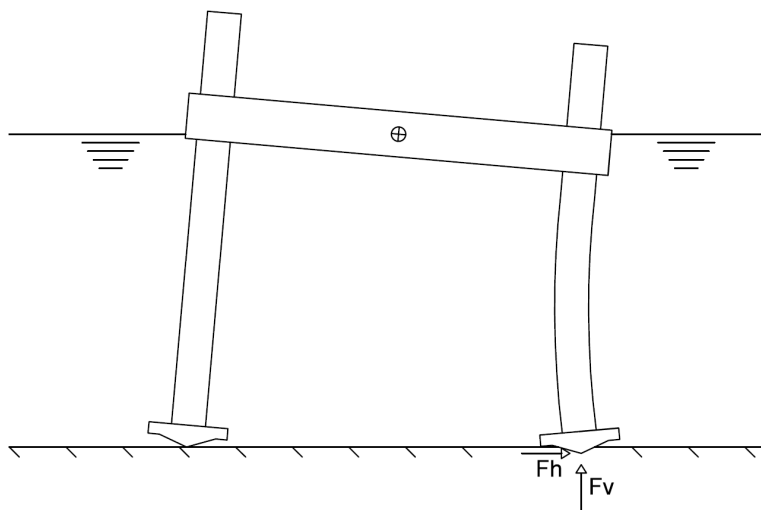


Figure 1.2 Schematic figure of impact between the spudcan of a SEU and the seabed. F_h and F_v are the horizontal and vertical forces, respectively, acting on the spudcan as a result of the impact.

The interest in these operational modes and their limitations is increasing as the number of SEUs employed within the offshore wind business is growing. The operation profile for a SEU employed within the offshore wind industry and one employed within the offshore oil and gas industry is different in some important

aspects. Generally, SEUs in the offshore oil and gas industry are used for exploration drilling where time on location may be as much as several months. A SEU used for installing wind turbines may spend as little time as a day on one location. Consequently, this results in considerably more frequent occurrences of installation and retrieval phases. Increasing the weather window for these operations, thus shortening the waiting time due to harsh weather, has a pronounced positive effect on the economic feasibility of using SEUs for installation and maintenance of wind turbines in particular and the competitiveness of offshore wind in general. Prognos AG and Fichtner Group (2013) identified both maintenance and operating cost and installation cost of offshore wind to be two of the top four areas with the greatest cost reduction potential in the life cycle of an offshore wind power plant. Offshore wind increasing its competitiveness against conventional energy resources such as coal and oil helps to increase the rate at which fossil fuel is exchanged against more sustainable energy resources. On these grounds, Statoil ASA as an offshore windfarm owner and manager expressed an interest in learning more about the physics governing the limitations of the operations and how this can be accurately modelled.

The objective of this thesis is to develop a method of analysis by which it will be possible to make weather window assessments for the installation and retrieval phases of a SEU. The method of analysis will take site-specific parameters, defined as soil type and water depth, into account in addition to vessel-specific and environmental parameters. The inclusion of site-specific parameters is the novel contribution compared to assessment methodologies used in practice today. The method of analysis will include the possibility of making assessments using different evaluation criteria, while the assessments in this thesis are limited to a structural evaluation criterion. The method of analysis will be tested and evaluated. Using the developed method of analysis, a study will be conducted with the aim of learning more of the physics behind and the sequence of events during an impact as well as investigating the necessity of including site-specific parameters in such assessments altogether.

1.3 Methodology

The task at hand is multidisciplinary, requiring knowledge of hydromechanics, structural mechanics and impact mechanics (including geomechanics). Existing theory in the fields of hydromechanics and structural mechanics are well capable of describing the scenario, whereas the soil-structure interaction during impact is a relatively novel area. To address this, a literature study with the purpose of finding one or combining several existing impact theories capable of describing the soil-structure interaction during impact is conducted.

To address the objective of this thesis a simulation model, see Figure 1.3, is built that handles not only vessel and environmental parameters but also site-specific parameters. The main output from the model is an estimate of the weather window. In this thesis, the evaluation criterion with which the weather window assessment is performed is a purely structural criterion. The structural capacity of the vessel is its capacity against failure for a load acting in a certain point. In this thesis, the structural capacity is evaluated using only yielding and buckling criteria and should thus not be confused with the integrity of a structure that generally also includes more criteria such as fatigue and fracture evaluations. Still, the developed methodology supports other evaluation criteria to be used. The model comprises three submodels dedicated to different tasks within the simulation model:

- A hydrodynamic submodel for simulation of vessel motion in waves. Simulations are performed in the time-domain.
- An impact submodel for simulation of soil-structure interaction during impact. The theoretical model from the literature study will be used for describing this interaction and is implemented into the time-domain simulations using existing functionality.
- A structural submodel for evaluating necessary structural criteria for the vessel design. Evaluations are performed using FE analysis.

The submodels in the simulation model are verified in order to ensure behaviour as expected in time-domain and FE simulations. The hydrodynamic and structural models are verified against analytical expressions for eigenperiods and analytical beam theory, respectively. The impact submodel is verified against the theoretical framework that it is based on. Only the geotechnical part of the impact submodel is verified. No verifications against measurements from reality are performed.

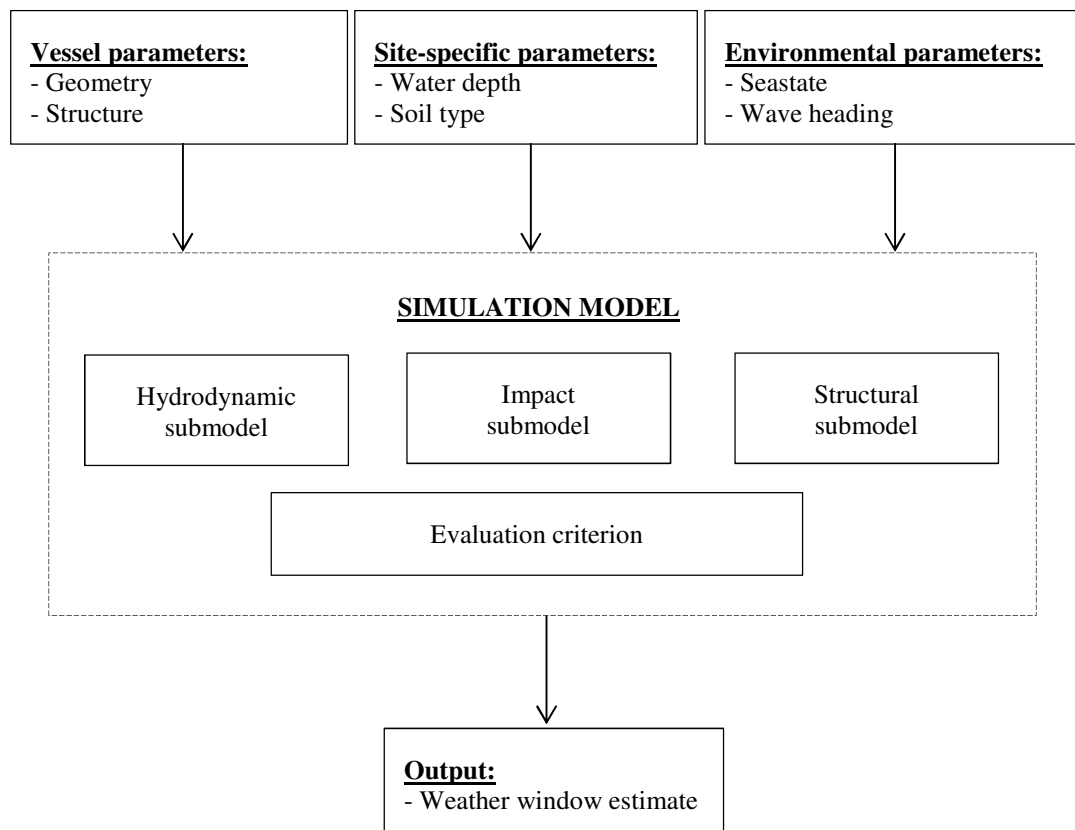


Figure 1.3 Flowchart visualizing input parameters, simulation model with submodels and output from the simulation model.

A case study is performed applying the simulation model using an existing vessel design. The case study aims at studying how the impact forces vary with soil type, heading, wave period, significant wave height and how they compare to impact forces calculated by the recommended practice by DNV (2012) as a comparative measure. The case study will also study how the structural capacity varies with the direction of the loading in the horizontal and vertical direction. A weather window estimate based on obtained impact forces and calculated structural capacity is the final outcome of the case study. The case study is also used as a base for evaluation and discussion of the proposed method of analysis.

Several softwares have been used in this thesis. Below, a short presentation of each one of them is given:

Hydrodynamic/Impact analysis

- The hull model was created using MULTISURF version 8.2, see AeroHydro Inc. (2011). MULTISURF is a computer-aided design (CAD) software aimed at marine implementations.
- Hydrodynamic properties for the hull model is extracted using the numerical tool WAMIT version 7.05, see WAMIT Inc. (2013). WAMIT is based on a three-dimensional panel method and is used for analyses of surface wave interaction with offshore structures.
- Time-domain simulations are performed using SIMA version 1.10.0.6079 and SIMO version 4.1.4, see MARINTEK (2013a) and MARINTEK (2013b). SIMO is a numerical tool for simulation of marine operations in the time-domain and is part of the SESAM package as provided by DNV. SIMA is a graphical interface used on top of SIMO. The simulations are non-linear and may thus include non-linear effects such as reaction forces from the seabed and drag and inertia forces.

Structural analysis

- The structural model was partly built in AutoCAD 2014. Autocad is a computer-aided design software for 3D-modelling. See Autodesk(2013).
- Finite element analyses and some of the modelling are performed using the FE software ABAQUS/CAE version 6.13. ABAQUS is a software for finite element analysis and is used within several fields of engineering, i.e solid mechanics, fluid mechanics and electromagnetics. See Dassault Systèmes (2013).

Postprocessing

Post-processing is mainly done in MATLAB version 2012b (8.0.0.783), see The Mathworks Inc. (2012). Some post-processing is also done using in-house scripts.

1.4 Limitations

The methodology developed and presented in this thesis is implemented in a simulation model that is built around one existing vessel design. Thus, the results obtained from the case study are not necessarily applicable to other vessels. The area of operation for this specific vessel is primarily the North Sea, thus wave data from this area is used in the thesis. The hydrodynamic simulations are performed in the time-domain in order to incorporate the impact and seafloor interaction in the same simulation. The water depth for all calculations is chosen as 35 metres, which is a representative depth for locations used for bottom-fixed offshore wind turbines.

Impacts are studied as a phenomenon caused by vessel motion in waves. Other environmental loads, such as current and wind that might affect the impact, have not been considered. The impact itself is limited to the time-intervals when the spudcan penetrates the seabed, i.e. has a downward speed. During impact, only permanent (plastic) deformation of the seabed is accounted for and no load history is accounted for in the soil implying that every impact is “new”. Elastic deformation is assumed to be small and has therefore not been considered. Also, the seabed is considered to be flat and homogenous. Generally, seabeds are not flat and consist of several layers with different characteristics. This assumption means that the punch-through

phenomenon has been disregarded altogether and that all four legs have the same length in any given simulation. In the time-domain simulations, including the impact analysis, rigid hull motion of the vessel is assumed to be valid. Furthermore, no depth-dependency of hydrodynamic coefficients is considered even though the proximity of the spudcans to the seabed is obvious and the effects could be noticeable. The loading rate during impact suggests that strain-rate effects can be dominant. Strain-rate effects on soil deformation behaviour are, however, omitted since studies on the topic suggests small but rather varying effects. The method of analysis accounts for all four spudcans. However, they are treated together in the post-processing and information on interaction between the spudcans and which ones are experiencing the worst impact has been disregarded.

The limiting criterion considered in this thesis is the structural strength due to certain evaluation criteria. Other possible factors that could limit the weather window for installation and retrieval of an SEU is disregarded. All structural evaluations are performed using FE analysis on one leg and one spudcan from the case vessel. The jackhouse is not accounted for in the evaluations and the leg is considered as rigidly fixed to the hull. The simulations are quasi-static meaning that no dynamic effects are accounted for in the structural capacity. Consequently, no strain rate effects of the structural members are regarded. Welds are not taken into account in the structural analysis assuming no residual stresses. The structural capacity is in this thesis defined as the strength against failure caused by yielding and buckling in the structure. Fatigue and brittle fracture governed by impact loads is hence disregarded completely. Furthermore, no safety margins are applied on the structural capacity while assessing the weather window. Application of loads on the FE model is done on the entire bottom plating of the spudcan assuming full penetration during the entire impact. The loads are also simplified to two dimensions for each wave heading as it is believed that horizontal loads transverse to the incoming waves will be relatively or very small. For example, in head waves the only forces considered are in the longitudinal-vertical plane of the vessel.

1.5 Outline of thesis

Section 2 gives a general introduction on impact mechanics followed by a section on soil mechanics and theories describing impact in soil. A theoretical model to be used for soil-structure interaction between spudcan and seabed is presented.

Section 3 describes the simulation model in detail including the case vessel followed by a verification of the submodels presented in Section 4. The procedure used in the case study is presented in Section 5 and the results are presented in Section 6.

Section 7 discusses the results and conclusions drawn during the work with this thesis are given in Section 8. Recommendations for further work on the topic are given in Section 9.

2 Impact mechanics

In general, an impact may be described as a collision-like event where high forces are acting over a relatively short period of time. Impact scenarios are of interest for predicting the behaviour of colliding objects in a macroscopic perspective (accelerations, kinetic energy, etc.) and for predicting possible elastic and plastic deformations of the objects. In this thesis, impact is defined as the time interval when the spudcan of the SEU penetrates the seabed vertically. Sliding in the horizontal plane that occurs outside this time interval does not belong to the impact and is considered as a separate phenomenon. Impact forces are subsequently defined as the forces, horizontal and vertical, acting on the spudcan from the seabed during the impact.

Impact between spudcans and seabed will occur due to motions of the SEU caused by waves. The impact force occurring during such an impact is dependent on the energy contained in the impact and how this energy is absorbed by the colliding bodies. The main factors affecting the energy content of such an impact are identified by Chakrabarti (2012) as:

- *Wave height and wave period.*
- *Vertical and horizontal velocity of the spudcan prior to impact relative to the seabed.* These motions are comprised of wave-induced motions of the vessel and jacking velocity of the leg. However, the jacking velocity is comparatively small and can be neglected. Hull hydrodynamic characteristics and viscous leg damping, which in turn is dependent on leg length, governs the wave-induced vessel motion for a specific seastate.
- *Inertia of the vessel.* Based on both structural and hydrodynamic mass of the vessel.

DNV (2012) gives guidelines for analysis focused on the impact force between a leg and the seabed when installing a SEU. The relative velocity between the leg and seabed is assumed to be governed by pitch and roll motions only. It is presented as a simplified method with the following conservative assumptions:

- All energy present in the impact is absorbed by a single leg.
- The lower end of the leg is stopped immediately when the leg touches the seabed.
- The seabed is infinitely rigid.

The entire impact energy is assumed to be absorbed by the spudcan, leg and jackhouse. The magnitude of the forces will thus depend on wave conditions, water depth, structural parameters and leg location (with regard to centre of flotation). The horizontal and vertical contributions to the impact force are then written as:

$$F_{Horizontal} = \frac{2\pi}{T} \theta \sqrt{\frac{I_m k_H}{\left[1 + \frac{k_V}{k_H} \left(\frac{d}{h}\right)^2\right]}} \quad (2.1)$$

$$F_{Vertical} = \frac{2\pi}{T} \theta \sqrt{\frac{I_m k_V}{\left[1 + \frac{k_H}{k_V} \left(\frac{h}{d}\right)^2\right]}} \quad (2.2)$$

DNV thus limits the analysis by incorporating a mechanical model describing only the structural members of the leg, assuming the seabed to be infinitely rigid. This is believed to produce large estimates of impact forces as the energy-absorbing characteristics of the seabed are disregarded altogether. In this section, a literature study of existing impact theories is carried out with the aim of establishing a theoretical model predicting forces arising from an impact between spudcan and seabed incorporating soil deformation behaviour. The investigation aims not to produce a new theory but to find a model capable of describing the soil-structure interaction by using one or combining several existing theories. Focus is put on impact mechanics in general and impact in soil in particular, as it is believed that knowledge of soil deformation behaviour is of paramount importance.

2.1 Classical mechanics approach

In classical mechanics (Goldsmith, 1960), the term collision is used for the physical phenomenon of large sudden accelerations caused by high forces over relatively short time periods. Momentum is conserved in all types of collision, whereas the kinetic energy is not. Three different scenarios are of importance:

- Perfectly elastic collision, where no energy dissipates due to non-elastic behaviour and thus, the kinetic energy is conserved throughout the collision.
- Inelastic collision, where energy dissipates due to non-elastic behaviour and the kinetic energy is not conserved throughout the collision.
- Perfectly plastic collision, a special case where the two bodies colliding stick together after the collision. This is the type of collision where the kinetic energy of the system is reduced maximally.

The difference in conservation of kinetic energy is taken into account by a coefficient of restitution. The coefficient of restitution is a positive real number between 0 and 1 where the case of 0 represents a perfectly plastic collision and the case of 1 represents a perfectly elastic collision.

Mathematically, this approach is very appealing and from a macro-perspective it is fully functional. However, it cannot predict forces on the objects during the collisions and neither can it say anything of the stresses arising within the bodies.

2.2 Contact mechanics approach

Stresses arise in bodies as a result of impact forces acting on them throughout a collision and the classical mechanics approach is not sufficient for determining such properties. Instead, the interaction of items with inherent properties such as stiffness and damping may be modelled as a spring-damper system. This is the extension of the Hertz contact theory presented in 1880 where Hertz related the contact force between two colliding bodies with the deformations and the elastic moduli of the bodies. This approach assumes the deformations to be elastic and is thus not suitable for use in scenarios where large plastic deformations are likely to occur. However, dynamic behaviour of structural members is generally well described by contact mechanics. A simple single degree of freedom (SDOF) spring-damper system is shown in Figure 2.1. A SDOF system consists of a spring representing the stiffness (k) of the model and a dashpot representing the damping (c) of the model. The equation of motion for such a system may be written as

$$m\ddot{x} + c\dot{x} + kx = F(t) \quad (2.3)$$

where $F(t)$ is a time-dependent force exciting the system.

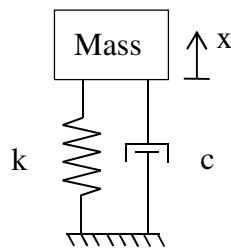


Figure 2.1 A schematic of a single degree of freedom (SDOF) system.

Several SDOF systems can be combined in order to express higher degree of freedom systems that better represent reality. A prerequisite for such a model is the properties of the items modelled. For linear, elastic materials such as steels these properties are well-known while for other materials, such as soils, etc., they may be difficult to define.

2.3 Impact in soil

Geotechnical engineering is mainly focused on static loading linked to the construction of buildings, bridges, etc., and the response of the foundation is considered over a long or very long period of time. Analyses of dynamic loads are usually restricted to vibration analysis of building foundations or similar analyses. These are usually based on the assumption that the foundation may be described by contact mechanics as an equivalent spring-damper system with mainly elastic deformations (Verruijt, 2012). An impact scenario, however, is a collision-like event where high forces are acting over a short period of time and large plastic deformations are likely to occur. The models used in conventional geotechnical engineering are thus not directly applicable. Instead, this section focuses on theories used in cone penetration tests (CPT) of soils as they are aimed at scenarios where large penetrations occur. This is preceded by a brief introduction to soil mechanics.

2.3.1 Soil mechanics

Soil is defined as the loose part of the earth's crust and it is built up by grains together with gas or water or a combination of the two. Within geology different soil types are defined by the size of the grains and this in combination with the amount of water or gas in the soil will affect its mechanical properties (Sällfors, 2009). As this thesis treats the soil on the seabed it is assumed that it is undrained and voids between the grains is filled up entirely by sea water. Two common seabed fractions, sand and clay, are studied closer as their internal mechanism is important to understand their mechanical properties.

Sand is usually described as a soil where the grain diameter is between 0.2 and 2 mm. These are the smallest fractions where the microstructure is still visible to the naked eye. As the internal mechanics of sand is dominated by friction forces between the grains it is possible to describe the strength of the material using the internal friction angle ϕ . The angle can be described as the angle of the cone that will occur if the sand is put in a pile. When this angle is exceeded, shear forces will create a slide in the sand. Most sands have an internal friction angle between 20 and 40 degrees where a larger angle corresponds to harder sand.

Clay, on the other hand, is built up by grains with a diameter smaller than 2 μm . This means that the micro-structure is invisible to the eye and the clay is perceived as a homogenous matrix. The grains are often leaf-shaped and connected with complex chemical connection forces, which means that the internal friction force is not dominating the mechanics of the material. The strength of clay is instead described by its shear strength that is tested in the field, and high shear strength corresponds to a harder clay (Sällfors, 2009).

2.3.2 Cone penetration test

Vertical penetration of soil by cones has been quite thoroughly studied as it is a frequently used procedure for in-situ testing of soils to determine properties and stratification (layering). During the test, a rod with a conical base is pushed into the soil at a constant controlled rate and continuous measurements are carried out of the resistance to penetration, both from frictional forces acting on the cone tip and along the rod as it is pushed into the ground, see Figure 2.2.

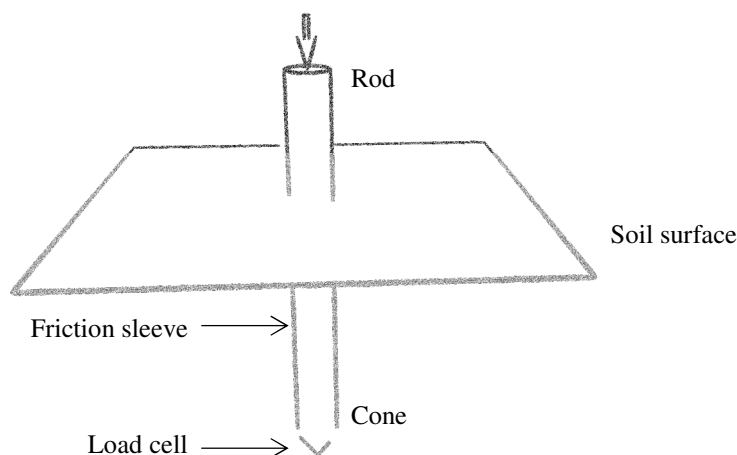


Figure 2.2 Schematic showing the setup of a cone penetration test.

Consequently, if soil parameters and layering are known it is possible to predict the resistance that the cone will have to overcome in order to achieve penetration. According to Mitchell and Brandon (1998) five different approaches exist for obtaining cone resistance correlations for such a setup:

- Bearing capacity theory, based on the assumption that the penetration resistance of the cone is equal to the collapse load of the soil it penetrates. The collapse load or the ultimate bearing capacity is defined as the maximum average contact pressure between the penetrating object and the soil which does not produce shear failure, i.e. plastic deformation. Soil stress-strain and volume change behaviour is not accounted for explicitly in the bearing capacity theory (Mitchell and Brandon, 1998).
- Cavity expansion theory, makes use of the proportional relationship between the pressure needed to produce a deep hole and the pressure needed to expand a cavity of the same volume in an elastic-plastic material, first presented by Bishop et al. (1945). It has been found to produce more realistic results than the bearing capacity method partly because it accounts for both elastic and plastic deformation during the penetration (Mitchell and Brandon, 1998).

- Steady-state deformation theory, defined as the state where a soil deforms without change in deformation velocity, volume, effective stress or shear stress. It could be used for producing idealized stress-strain curves for a soil and thus predict the resistance towards penetration (Poulos, 1971).
- Incremental finite element analysis, using a large strain FE formulation that is capable of generating a correct stress field around the cone. Predictions of cone resistance can then be made (Walker and Yu, 2006).

Calibration chamber testing, cone penetration tests are made in closed chambers on soils where soil type, density and both vertical and horizontal stresses are well known throughout the test. From such tests, resistance curves for the tested soil type are given (Houlsby and Hitchman, 1988).

2.4 Concluding remarks

As the materials as such in the structure and in the seabed behave very differently, it is believed that a theoretical model describing the impact scenario should be split into two elements connected in a series: one element for describing the structural deformation behaviour and one element describing the soil deformation behaviour. A spring-damper system is believed to be a sufficiently accurate description of the structural deformation course during an impact, as the model to be used in this thesis does not need to handle plastic macro-deformation of structural members due to the fact that this is not what the simulation model is intended for. Seastates giving impacts smaller than the structural capacity lead to elastic-only deformations in the structural members. From the brief introduction on possible approaches for predicting penetration resistance in soil, it is obvious that the use of calibration chamber testing can be discarded for economic and practical reasons. Incremental finite element analysis would require knowledge of soil mechanics beyond the scope of this thesis and would also extend the computational effort required to estimate the impact force and has also been disregarded. As stated by ISO (2012), plastic deformation dominates during penetration of soil and thus a possible inclusion of an elastic representation of the soil may be disregarded, implying that the steady-state deformation theory and cavity expansion theory might be unnecessarily complicated to describe the impact scenario. The bearing capacity theory is the recommended theory to use by both ISO and SNAME in their respective guidelines, and it will be used for describing the deformation course of the seabed and for predicting the resistance to penetration from now on in this thesis. It is described more in detail in Section 2.6. Figure 2.3 shows a schematic picture of how a model taking into account elastic macro-deformation of structural members and plastic deformation in the seabed could be represented in 2 DOFs.

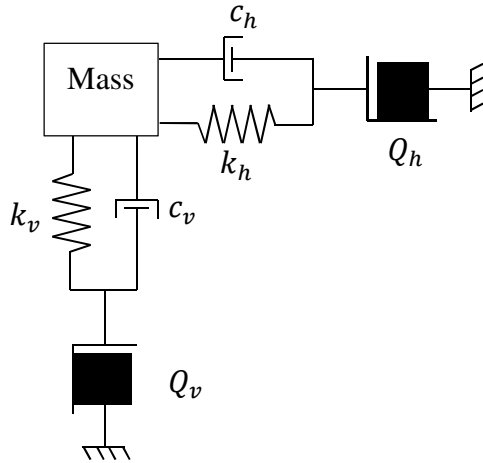


Figure 2.3 Schematic picture of an impact model showing spring with stiffness k and dashpot with damping coefficient c representing the structural members under consideration and a sliding frictional element with bearing capacity, Q , representing the seabed. Subscript h corresponds to the horizontal direction and subscript v to the vertical direction.

2.5 Bearing capacity theory

The recommended theory in ISO (2012) and a somewhat simplified version in SNAME (2008) for conical spudcans vertically penetrating the seabed is based on the bearing capacity theory and is presented below. ISO (2012) and SNAME (2008) also both recommend the same practice to be used for calculation of the resistance curves in the horizontal plane.

During initial penetration, i.e. penetration in previously undisturbed soil, plastic deformations dominate. The vertical load acting on the spudcan during penetration is proportional to the projected area of the spudcan in contact with the seabed. This is valid for spudcans of approximately conical shape where the projected area is a function of the penetration depth (ISO, 2012).

2.5.1 Penetration in clay

For foundations in clay of uniform shear strength the vertical bearing capacity can be expressed as:

$$Q_v = (\mu N_c s_c d_c + p'_o) \pi B^2 / 4 \quad (2.3)$$

The product $N_c s_c d_c$ is the bearing capacity factor and p'_o is the effective overburden pressure at penetration depth D_p . B is the diameter of an equivalent contact area. This expression is valid for cone angles between 60 and 180 degrees (a flat plate). The bearing capacity factor is dependent on the relative penetration depth, $\frac{D}{B}$, and tabulated values are available in ISO (2012).

Horizontal capacity of foundations in clay may be formulated as:

$$Q_h = C_H (Q_v - p'_o \pi B^2 / 4) \quad (2.4)$$

C_H is a depth dependent capacity coefficient relating the horizontal capacity to the vertical capacity.

2.5.2 Penetration in silica sands

For foundations in silica sand the vertical bearing capacity can be expressed as:

$$Q_V = \gamma' d_\gamma N_\gamma \pi B^3 / 8 + p'_o d_q N_q \pi B^2 / 4 \quad (2.5)$$

The parameters d_γ and d_q are depth factors and N_γ and N_q are dimensionless bearing capacity factors.

The depth factors are functions of the relative penetration depth, $\frac{D}{B}$, and the friction angle, ϕ . The dimensionless bearing capacity factors are functions of the friction angle, ϕ , and tabulated values are available in ISO (2012).

Horizontal bearing capacity of foundations in silica sands may be expressed as:

$$Q_H = F_V \tan(\delta) + \frac{1}{2} \gamma' (k_p - k_a) (h_1 + h_2) A_s \quad (2.6)$$

where δ is the friction angle between steel and soil, usually taken as $\delta = \phi - 5$. The parameters k_p and k_a are earth pressure coefficients and h_1 and h_2 are different embedment depth coordinates. A_s is the laterally projected area of the embedded cone. F_V is the actual vertical force acting on the spudcan at the time meaning that Q_H is not dependent on the vertical capacity but rather on the normal force revealing it as a frictional contribution.

2.5.3 Load rate effects on soil deformation behavior

As cone penetration tests are conducted ensuring a constant velocity of the rod, the theories developed to interpret the test data, described above, are also focused on rather slow and steady deformations. Their applicability to impact scenarios would then depend on if it is needed, and in that case how does one account for faster deformations. Danziger and Lunne (2012) presented a compilation of studies made on the topic of load rate effects on the bearing capacity of soils. Most of the studies showed a minor increase (~5 %) in bearing capacity with an increasing loading rate. However, a few studies also presented results suggesting that increased loading rates could actually decrease the bearing capacity. No concluding remark about the applicability of the results is given by Danziger and Lunne and no generally accepted approach for including rate effects have been found to exist. Thus, the bearing capacity theory as presented in this section will be used as it is, with no adjustments for rate effects.

3 Simulation model

The simulation model is split into three submodels as presented in Section 1.3 and visualized in Figure 1.3:

- A hydrodynamic submodel for simulation of vessel motion in waves. Simulations are performed in the time-domain.
- An impact submodel for simulation of soil-structure interaction during impact. The theoretical model from Section 2.5 is used for describing this interaction.
- A structural submodel for evaluating necessary structural criteria for the vessel design. Evaluations are performed using the FE method.

Figure 3.1 shows the interconnections between the submodels. The hydrodynamic as well as the impact submodel is integrated into SIMO, see MARINTEK (2013a) and MARINTEK (2013b), where a coupled non-linear time-domain analysis is performed. Possible inputs to time-domain simulations are seastate, soil-type, wave heading and water depth. Outputs are time-series of forces between the spudcan and the seabed. The structural submodel comprises an FE model built in ABAQUS, see Dassault Systèmes (2013), on which quasi-static analyses are performed to obtain the capacity of the structure that is being investigated. Note that the structural submodel is a stand-alone module and is not directly coupled to the time-domain analyses of the impact forces. This is a time-efficient approach compared to the straightforward way being of applying the time-series of impact forces directly on the FE model in a fully dynamic analysis.

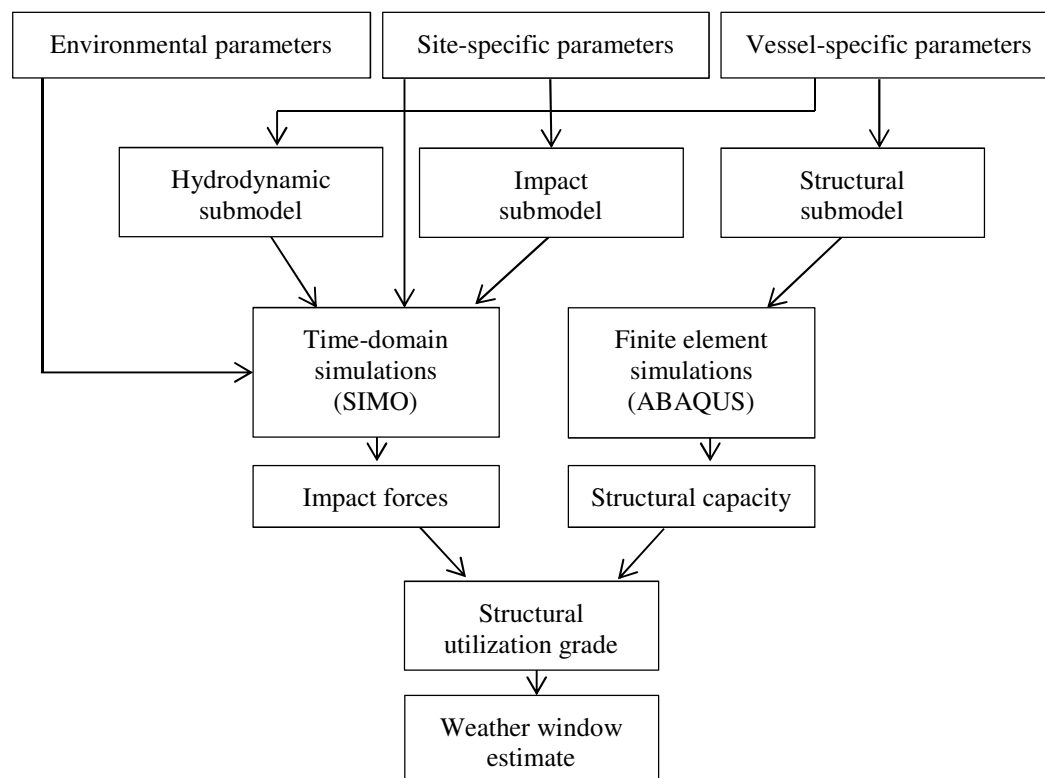


Figure 3.1 Flowchart visualizing interconnections between submodels and the simulation paths.

Eventually, impact forces are compared to the structural capacity to obtain utilization grades of the structure and a weather window estimate. The impact forces and structural capacity are considered to be two-dimensional for a fixed incoming wave heading. For example, impact forces and structural capacity are considered to be two-dimensional in the longitudinal-vertical plane of the vessel if the vessel is subjected to head seas, and, consequently, impact forces and structural capacity are considered to be two-dimensional in the transverse-vertical plane of the vessel if the vessel is subjected to beam seas. These planes are henceforth in the report referred to as loading planes. An attempt to visualize these planes is made in Figure 3.2.

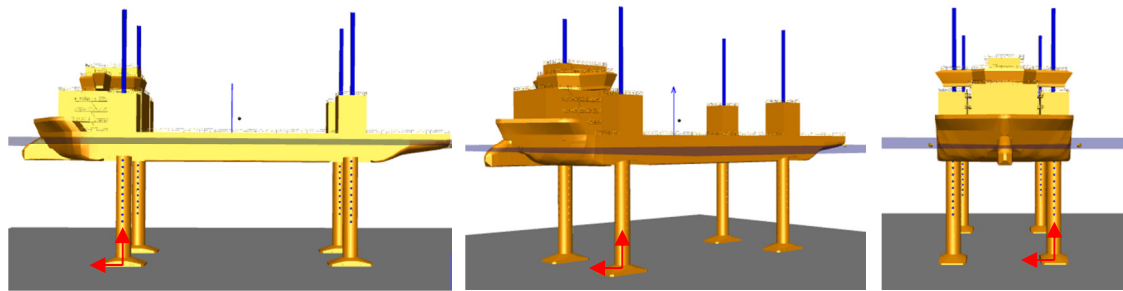


Figure 3.2 Loading planes for incoming wave headings 180 degrees (leftmost figure), 135 degrees (middle figure) and 90 degrees (rightmost figure). Waves are incoming from the left edge in all three figures. The red arrows in the figures represent the horizontal and vertical forces acting on the spudcan in the plane of the incoming waves. An external hull geometry file is used for visualizing the vessel. Courtesy of Fred. Olsen Windcarrier AS.

The simulation model is constructed based on a jack-up vessel of the Gusto MSC NG-9000C-HPE type. Length overall is 132 m, breadth is 39 m and moulded depth is 9 m. The ship's lightweight (including legs and spudcans) is almost 1,5000 tonnes. The vessel is self-propelled and designed for multi-purpose use but is widely used for wind turbine installations, see Figure 3.3. The vessel features a DP2 system. The vessel has four cylindrical legs, 74.2 metres long and 4.5 metres in diameter, enabling operation in water depths up to 45 metres. The aft port leg is equipped with a "around the leg" crane that is used for loading and installing operations. The crane is shown in Figure 1.1. The spudcan is a rectangular shaped steel structure with a bottom area of 106 m² (Drydocks world, 2010). The jackhouse, where the leg is attached to the hull, is constructed as hydraulic pistons holding the leg in a vertical direction and guides to absorb horizontal forces. The jacking capacity is 5,300 tonnes implying that it can elevate the hull using this load on each leg. The holding capacity on, the other hand, is the operational limit that the jacking system can hold and that is 9,000 tonnes (Drydocks world, 2010).

The loading condition used for the simulation model is a representative loading condition for a typical wind turbine installation project as conducted by the Gusto MSC NG-9000c-HPE type vessel. Eight bottom-fixed wind turbines are to be installed on a site where the bottom foundations are already in place. The installation thus includes eight towers, eight nacelles and hubs and 24 blades (for three-bladed turbines), see Figure 3.3. The total displacement of the ship is almost 22,000 tonnes at a draft of 5.2 m in this condition (Fred. Olsen Windcarrier AS, 2014).



Figure 3.3 *Gusto MSC NG-9000C-HPE, in transit fully loaded. Courtesy of Fred. Olsen Windcarrier AS.*

3.1 Hydrodynamic submodel

A hull model based on the geometry of the case vessel, produced in MULTISURF, see AeroHydro Inc. (2011), is used as input to WAMIT, see Wamit Inc. (2013), where force transfer functions, hydrostatic stiffness, added mass and damping in the form of retardation functions for the vessel are calculated for the loading condition described above and used as input to the modelling in SIMO. Figure 3.4 shows the calculation domain in SIMO including the model of the vessel. In addition to hydrodynamic data, a mass model is required in the form of a mass matrix and a damping matrix. Hydrodynamic mass of hull, legs and spudcans is added to the mass matrix. Viscous damping of legs and spudcans are calculated by the Morison equation, in accordance with the general recommendations in DNV (2013) and recommended practice in DNV (2012), and added to the damping matrix. The vessel is constrained by a horizontal anchor system to keep it stationary, possible effects from this setup on the vessels non-horizontal motions in waves are disregarded. Details of the hydrodynamic model may be found in Appendix A.

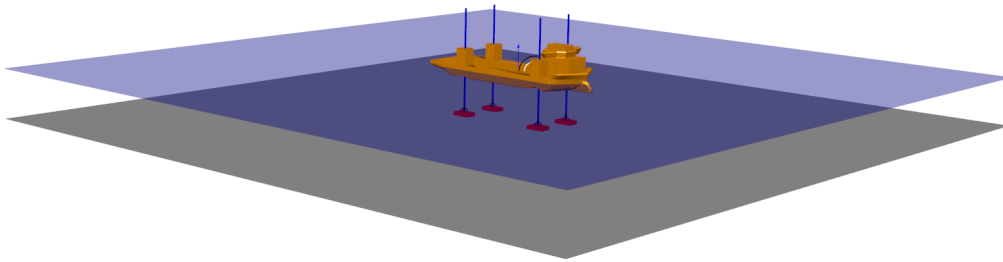


Figure 3.4 Calculation domain in SIMA/SIMO. Hull model visualized by an external geometry file, courtesy of Fred. Olsen Windcarrier AS. The blue sticks represent the legs and the red boxes represent the spudcans.

3.2 Impact submodel

Flexibility of the legs is accounted for, as part of the impact model described in Section 2.4, by introducing couplings between spudcans and legs in the model with stiffness extracted from the structural submodel that is described in Section 3.3. Stiffness proportional damping is utilized in these couplings. According to DNV (2012), structural damping is expected to be 1-3% of the structural stiffness. Here, 1% is used in the axial direction. To stabilize the simulations, 5% are used in the transverse direction.

Based on the theory presented in Section 2.5, tabulated values of bearing capacity of sand and clay are calculated and implemented in the time domain simulations. These are based on the geometry of the penetrating spudcan in intervals of ~5-10 cm. For a seabed consisting of rock the same model as for sand is used, but with comparatively very high capacities to avoid penetration of the seabed. When exported to SIMO, these tabulated values are interpreted as piece-wise linear functions and a fully plastic model is utilized in the SIMO soil penetration feature, explained in depth below.

3.2.1 The SIMO soil penetration feature

The soil penetration model is an in-built feature in SIMO. It uses depth-dependent resistance forces counteracting the motion of the penetrating object to imitate seabed behaviour. Three modelling options are possible when using the feature:

- The penetrating object causes no pressure to build up in the soil so that soil resistance against vertical motion is from sleeve friction and cone friction forces only. No horizontal motion is allowed.
- The penetrating object has valves letting water pass through during penetration. After a predefined time, it is possible to close the valves and apply a negative pressure. Designed for modelling of suction anchors. No horizontal motion is allowed.
- Same as the first option, but horizontal motion is allowed counteracted by a depth-dependent horizontal capacity.

In this thesis, the third option is used. See MARINTEK (2013b) for more information about the soil penetration model in SIMO.

3.3 Structural submodel

Geometrical modelling has been performed partly in AUTOCAD, see Autodesk (2013), and partly in ABAQUS. The simulations are undertaken using the FE solver in ABAQUS. The FE model consists of one leg and one spudcan, represented by properties corresponding to the arrangement used on Gusto MSC NG9000C-HPE as described in Section 3. Details of the structural arrangement are provided by Fred. Olsen Windcarrier AS. However, they are subject to confidentiality and will not be presented in this thesis. The modelling is performed in accordance with the guidelines set by ISO (2012) and DNV (2012) and is briefly presented below.

In this thesis, the leg is modelled as a detailed model using shell elements to represent the geometry. It is built up by a steel tube with a diameter of 4.5 metres pierced with holes for the jacking pistons. The holes are placed on four sides of the leg on equal intervals throughout the length. The lower part of the leg ends up in the spudcan. The tube runs through the spudcan structure and rests on the bottom plate as seen in Figure 3.5. The spudcan model is built up by a number of bulkheads that are attached to the lower part of the leg. The bulkheads are vertical plates that radiate from the centre of the spudcan. The inside of the leg is supported with hexagonshaped bulkheads encircling the centre. The skin plating comprising the outer shell of the spudcan is stiffened with T-profile stiffeners at the top and bottom. The bottom is a rectangular flat plate with a pyramidal immersion in the centre quadrat. A figure of the model with a cut is shown in Figure 3.5. The spudcan is modelled using shell elements to represent all the structural members. Welds are not accounted for in the model.

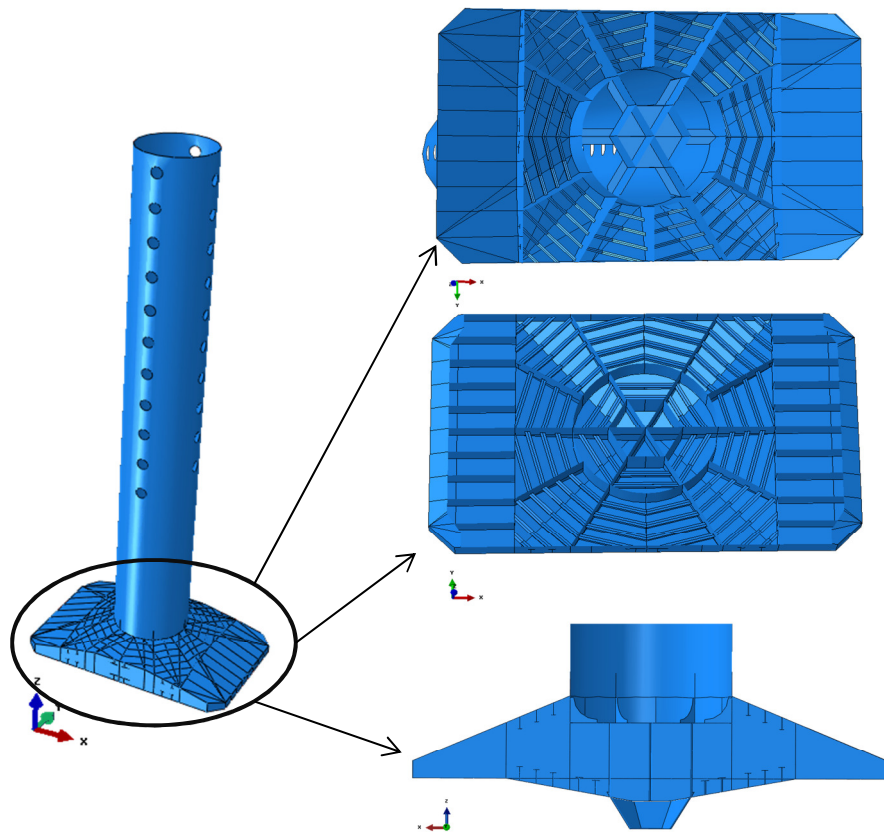


Figure 3.5 The geometry model of the leg and the spudcan.

3.3.1 Mesh

The meshing is performed using the automatic mesh tool in ABAQUS in which it is possible to control the number of elements by seeding edges with a desired distance between nodes. This operation can be done either globally for the entire model or locally for certain edges where a finer mesh is desired. The model is primarily meshed using quadrilateral (S4R) elements, but some triangular (S3R) elements are used to accurately describe the geometry.

An initial mesh is generated using a global seed with 0.1 metres between the nodes along the edges. The initial global seed is chosen so that the stiffeners in the spudcan are represented with two elements along the width of the flange and four elements over the height of the web. The generated mesh is then used to find critical areas for different loading conditions. As this thesis uses a structural evaluation criterion that incorporates only yielding and buckling, these criteria will also be used as mesh convergence criteria. This means that the mesh needs to be evaluated with regard to two different criteria. For each region identified as critical the mesh is refined until a converged solution is reached using local seed along edges around the area. The number of elements needed for a converged solution differs between the two different evaluation criteria and thus the meshes will be converged separately.

The convergence study of the meshes shows that there are two regions on the model that need a refined mesh. The edges of the holes in the upper part of the leg is sensitive to horizontal forces as they will cause stress concentrations that are of interest, see no 2 in Table 3.1 and Figure 3.6. When subjecting the model to vertical loads there will be stresses in the top plate of the spudcan, see no. 3 in Table 3.2 and Figure 3.6. In order to save computational time the bottom and side plates of the spudcan are seeded with a coarser seed without any significant changes in the result. The results of the convergence study are displayed in Table 3.1 and the resulting mesh for yielding simulations is shown in Figure 3.6.

Table 3.1 *The local refined edge seeds in the critical regions and for buckling and yielding.*

	<i>Region</i>	<i>Yielding [m]</i>	<i>Buckling [m]</i>
1	Global model	0.1	
2	Edge of top holes in leg	0.01	0.05
3	Top plate of spudcan	0.05	0.1
4	Bottom and sides plate of spudcan	0.2	0.2

Hereafter, all results presented for yield strength are obtained using a mesh with 375,672 elements distributed over the model with varying density around the above presented critical areas. The buckling strength is evaluated using a mesh with 145,530 elements. The number of integration points through the thickness of the shell is set to 5. Around 98% of the elements are quadrilateral and the remaining 2% are triangular.

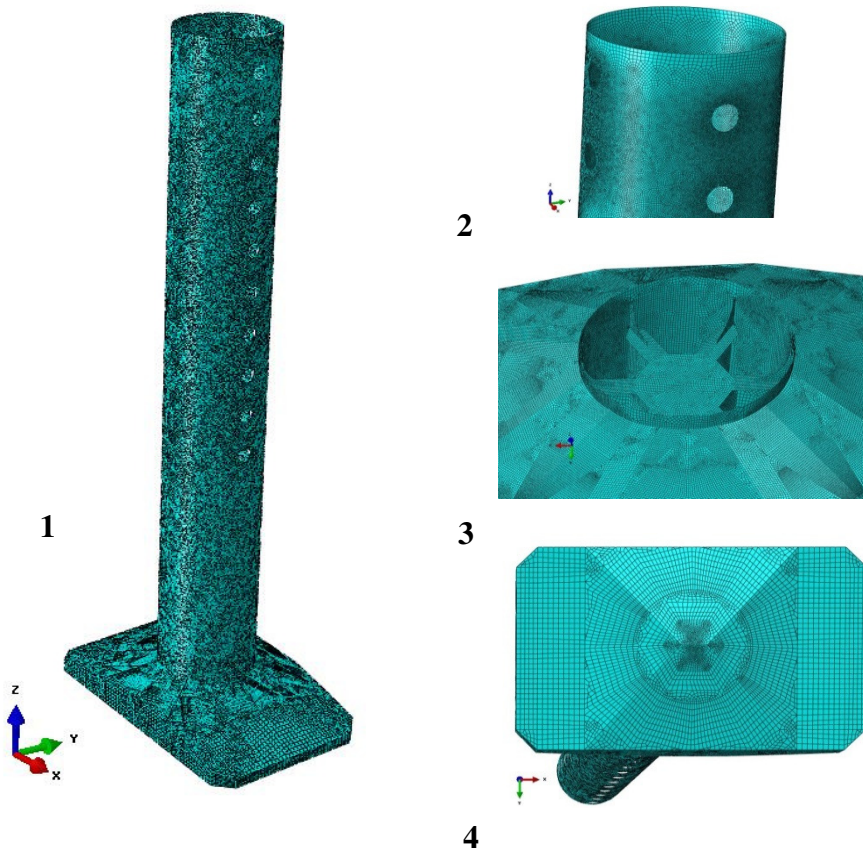


Figure 3.6 The generated mesh and areas with local seeds. The numbers in the figure correspond to the rows in Table 3.1.

4 Model verification

Verifications are needed to control that the submodels behave as expected when used in time-domain or FE simulations. The hydrodynamic and structural models are verified against analytical expressions for eigenperiods and analytical beam theory, respectively, whereas the implementation into the SIMO soil penetration tool of the geotechnical part of the impact submodel is verified against the theoretical framework that it is based on. No verification against measurements from reality is done. The focus is put on verifying the implementation of the geotechnical theory, i.e. the bearing capacity theory.

4.1 Hydrodynamic model

The geometrical hull model used in this thesis is an approximation of the underwater body of the real hull. The model is based on principal dimensions such as length overall, length in waterline, moulded breadth and draft for the specified loading condition. An initial guess based on visual judgment was followed up by iterative corrections of the geometry until displacement, GM and KM was within 1% of the real vessel for the loading condition described in Section 3.1.1.

To make sure that the hull model, when subjected to wave loads in the time domain, behaves as anticipated a comparison was performed between analytically calculated eigenvalues and eigenvalues obtained from letting the model oscillate freely in the time domain. The eigenperiod of a vessel, in a single degree of freedom, may be calculated as:

$$T = 2\pi \sqrt{\frac{m+m_a}{k}} \quad (4.1)$$

m is the mass of the vessel and m_a is the added mass in the current degree of freedom. k is the stiffness, also for the current degree of freedom. The analytic calculations are based on the hydrodynamic description of the hull, as presented in Appendix A. Table 4.1 shows the calculated and measured eigenperiods.

Table 4.1 *Eigenperiods for the hull model, analytically calculated and extracted from an oscillation test.*

<i>DOF</i>	<i>Eigenperiod [s] Analytically calculated</i>	<i>Eigenperiod [s] Oscillation test</i>
Heave	9.1	9.0
Roll	11.4	11.6
Pitch	8.1	8.7

4.2 FE model

There are structural members in the FE model that have simple geometries, which means that it is suitable for verification of local responses with an analytical beam theory in order to confirm the plausibility of the results from the FE analysis. This is done in the case of the leg, which is a steel tube pierced with holes. The FE model of the leg is verified by computing an analytical solution that is compared with the FE

result. The critical force in the vertical direction is calculated by assessing the force that corresponds to the first yielding response in the sides of the holes in the leg. The vertical capacity against yielding is estimated by:

$$F_{cr} = \frac{\sigma_y \times A_{steel}}{K_t} \quad (4.2)$$

σ_y is the yield strength for the material, A_{steel} is the nominal cross-section area of the steel in the leg and K_t is the stress concentration factor for a circular hole. The horizontal capacity against yielding is estimated by:

$$F_{cr} = \frac{M}{L_{leg}} \quad (4.3)$$

L_{leg} is the length of the leg and M is the bending moment at the fixed end of the leg, described by rearranging Naviers formula into:

$$M = \frac{\frac{\sigma_y}{K_t} \times I_{leg}}{R_{leg}} \quad (4.4)$$

I_{leg} is the moment of inertia of the leg and R_{leg} is the radii of the leg. All the formulas used here as well as cross-section properties and stress concentration factors may be found in KTH (2007). The results from the analytical and the initial FE simulations for the leg are shown and compared in Table 4.2. The verification reveals good resemblance between the results from the different methods of analysis for the leg.

Table 4.2 Structural capacity of the leg analysed using the FE model and analytical beam theory.

<i>Leg model</i>	<i>FE model</i>	<i>Analytical</i>
Vertical capacity	252 MN	270 MN
Horizontal capacity	8.8 MN	8.2 MN

The geometry of the spudcan is rather complex, not admitting easy verification by analytical beam theory, and hence no analytical calculations are performed.

4.3 Geotechnical verification

Only the geotechnical part of the impact submodel, i.e. the sliding friction elements in Figure 2.3 in Section 2.4, have been verified. The theory used for describing how the seabed responds during the course of penetration, i.e. the bearing capacity theory will not be verified as such. The theory is generally accepted and extensively used. Therefore, the verification is rather to study how well the bearing capacity theory is implemented into the SIMO soil penetration tool, as presented in Section 3.2.1. The study is conducted using only a single spudcan on which forces, velocities and motions may be present.

4.3.1 Vertical capacity

The vertical capacity, shown here as a function of depth, is obtained by letting the spudcan penetrate the seabed at a constant velocity and measure the force acting upon it from the seabed. Figure 4.1 shows the capacity for sand ($\phi = 35$ degrees) and clay ($s_u = 100kPa$) respectively.

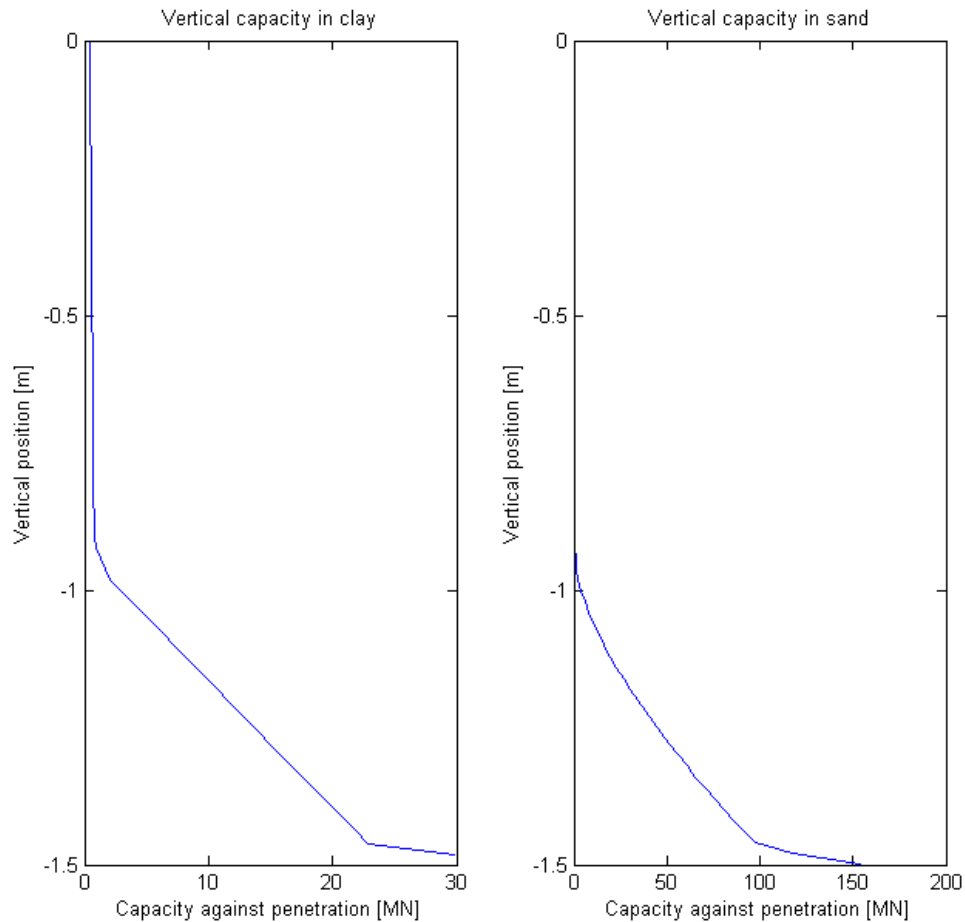


Figure 4.1 Vertical capacity [in MN] against penetration, as a function of penetration depth, in clay ($s_u = 100\text{kPa}$) and sand ($\phi = 35$ degrees).

The reaction forces from the seabed are of particular interest when the spudcan has already penetrated to a certain depth and when a force smaller than the capacity is applied. A test where the spudcan is subjected to forces with different magnitudes during finite time intervals was performed. The test is conducted by simulating 25 seconds during which four loading sequences are performed. During a load sequence, a constant external force is applied to the spudcan. All load sequences are 3 s long. The test is conducted using clay with a shear strength of 100 kPa to describe the seabed. Figure 4.2 shows the externally applied forces, reaction forces from the seabed and the vertical position of the spudcan side by side for the length of the simulation. The externally applied forces during loading sequences no. 1 and 3 are larger than any earlier applied force and thus result in additional penetration of the seabed. The externally applied loads during loading sequences no. 2 and 4 are smaller than earlier applied loads and thus results in no additional penetration. As a result of this, static equilibrium prevails during loading sequences no. 2 and 4, whereas dynamic equilibrium prevails during loading sequences no. 1 and 3.

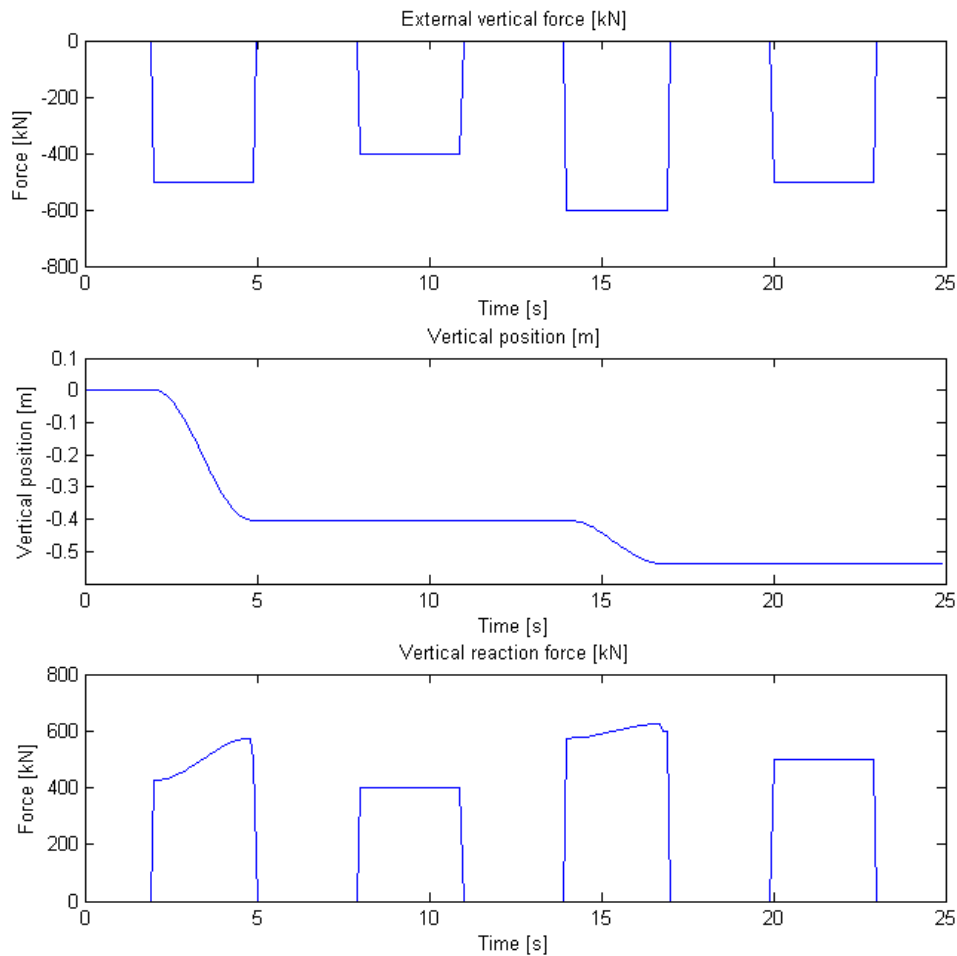


Figure 4.2 Reaction forces from the seabed and vertical position of the spudcan during a test where the spudcan was subjected to external vertical forces of different magnitudes during finite time intervals.

Thus, in the SIMO soil penetration tool the seabed has a fixed capacity against vertical loading for a certain penetration depth. If the load applied on the seabed exceeds the capacity, the penetration depth will increase until a level where the capacity is large enough to sustain the loading is reached. If the loading is smaller than the capacity, the penetration depth will remain unaltered while the reaction force from the seabed onto the penetrating object equals the loading, thus describing static equilibrium. As the deformation is plastic, there are no restoring forces acting on the penetrating object from the seabed if the penetration depth decreases due to motion of the vessel in waves. This behaviour is as expected from the bearing capacity theory.

4.3.2 Horizontal capacity

According to the bearing capacity theory, see Section 2.6, the horizontal capacity for sand and clay are not derived from the same phenomenon. In clay, the horizontal capacity is described by a proportionality factor against the vertical capacity, whereas the horizontal capacity in sand is described mainly by a friction term dependent on the actual vertical force instead of the vertical capacity.

In the SIMO soil penetration tool, however, the seabed is prescribed a fixed capacity against sliding in the horizontal direction for a certain penetration depth. If the horizontal loading exceeds the capacity, the penetrating object will start to slide in the horizontal plane, while the seabed exerts a counteracting – load with a magnitude equal to the capacity, and will remain to do so until either the loading decreases below the capacity or the penetrating depth increases due to increased vertical loading, thus increasing the capacity also against sliding. If the horizontal loading does not exceed the capacity, no sliding will occur and the reaction force on the penetrating object from the seabed is equal to the loading. Note that this way of describing the horizontal capacity is perfectly valid for clay but only valid for sand when the spudcan is moving downwards, i.e. penetrating the seabed vertically at the same time.

The test performed in the horizontal plane is identical to the test performed along the vertical axis, presented above, in all but two aspects:

- The test is conducted at a predefined, constant penetration depth, 0.7m, and all the forces act along the same line in the horizontal plane.
- The last two load sequences are negative loads, thus acting in the opposite direction.

Figure 4.3 shows the externally applied forces, reaction forces from the seabed and the horizontal position of the spudcan side by side for the length of the simulation. From Figure 4.3 the following can be observed:

- Reaction forces from the seabed are always equal to the capacity, irrespective of the magnitude of the externally applied force.
- Reaction forces from the seabed remain even after the removal of the externally applied force.

Naturally, the above implies the absence of force equilibrium and thus dynamic equilibrium should apply. This is also the case as output from the simulations registers accelerations proportional to the imbalances in force. However, output from the simulations also shows that there is no apparent change in velocity of the object. This is highly unphysical and thus the behaviour in the horizontal plane cannot, for any soil type, be regarded as expected according to the bearing capacity theory. Note that this is a shortcoming of the software and not the underlying theory. However, the horizontal forces are overestimated in all cases and accelerations and velocities are not used explicitly for calculation of results in this thesis implying that the horizontal forces as outputted from the simulations could serve as rough estimates. Also, as the time-periods studied in this thesis are comparatively short, the lingering horizontal reaction forces need not be a concern. Thus, the horizontal forces obtained throughout the simulations will be used in this thesis.

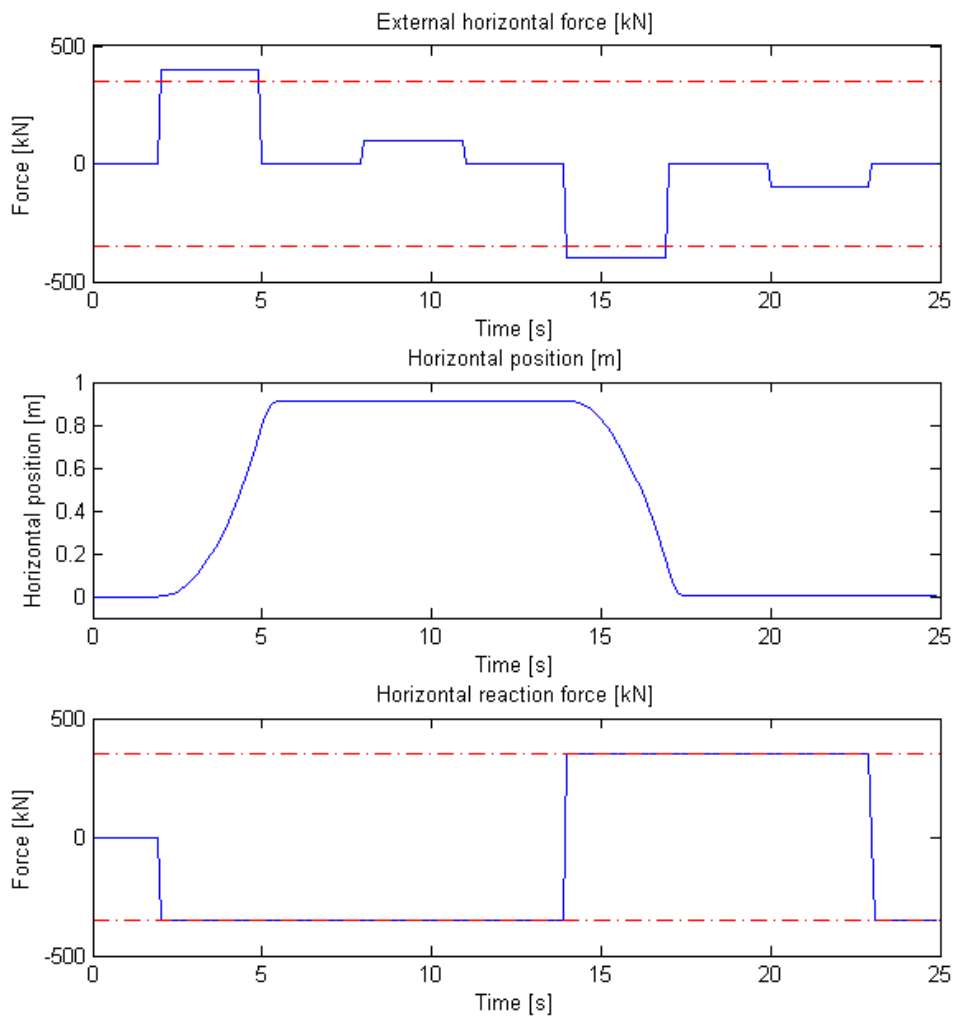


Figure 4.3 Reaction forces from the seabed and horizontal position of the spudcan during a test where the spudcan was subjected to external horizontal forces of different magnitudes and directions during finite time intervals. The red dashed lines show the horizontal capacity against sliding for the pre-defined penetration depth (0.7m).

5 Case study

A case study is conducted using the simulation model presented in Section 3. The case study comprises three different soil types and three headings of incoming waves, whereas water depth is kept fixed. Simultaneously, the recommended practice by DNV (2012), as presented in Section 2, is used for calculating impact forces as a comparative measure. The case study aims to:

- Study how the impact forces vary with the soil type, heading, wave period and significant wave height.
- Study how the structural capacity varies with the direction of the loading.
- Obtain a weather window estimate for a jacking operation. The purpose is to find an interval in the H_s/T_p -domain in which the case vessel can operate.

As visualized in Figure 3.1, two separate simulations are performed in this case study: one time-domain simulation, using the hydrodynamic and impact submodels to obtain impact forces, and one FE simulation using a model of a leg and spudcan to obtain the structural capacity. The input parameters and the simulation and post-processing procedure used for both time-domain simulations and FE simulations are presented in this section.

5.1 Time-domain simulation procedure

Simulations in the time-domain are of equal length of 3,600 s. The simulation length is limited to this length to keep the computation time manageable. A time step of 0.1 s is used with 100 subdivisions resulting in a minimum time integration interval of 0.001 s. The rather small time integration interval is necessary in order to resolve the large accelerations occurring during the impacts. The initial 500 time steps of each simulation are discarded. Input parameters that are varied between the simulations are heading [deg], significant wave height [m] and wave period [s]. Headings are chosen to include head sea (180 degrees), quartering sea (135 degrees) and beam sea (90 degrees), see Figure 5.1, as the direction of the vessel on location is not usually adjustable to the current environmental state.

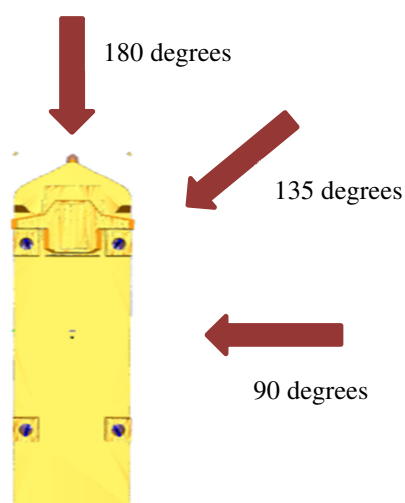


Figure 5.1 Incoming wave headings in relation to the vessel.

Seastates are chosen based on Metocean data for an offshore wind farm field in the North Sea (Statoil ASA, 2006). The significant wave height is varied from 1.5 m to

3.5 m in steps of 0.5 m and the wave period is varied from 4 s to 12 s in steps of 2 s. Simulations are carried out for all combinations of these wave heights and periods. Additionally, an extreme seastate ($H_s = 7 \text{ m}, T_p = 12 \text{ s}$) corresponding to only 0.03% of the wave statistics is simulated. As the wave periods are close to the eigenperiods of the vessel, see Section 4.1, the Pierson Moskowitz spectrum may not be used, see DNV (2012), and the JONSWAP spectrum is used instead.

Impact is simulated to a limited set of seabed characteristics chosen from commonly abundant seabed types on locations for offshore wind farms. Generally, seabeds consist of several layers with different characteristics. However, in this thesis it is assumed that the seabed consists of a single homogenous layer. Impacts to three different characteristics are simulated for seabeds consisting of:

- Rock
- Sand with an internal friction angle of 35 degrees
- Clay with a shear strength of 100 kPa

Additionally, impact forces are calculated using DNV's recommended practice, presented in Section 2.3, for all seastates as a comparative measure. The rocky seabed is simulated using the SIMO soil penetration tool with a resistance to penetration set as high as the stability of the time-domain simulation could allow. The final setting resulted in a "deformation" of the rock of about 2 cm for the largest impacts. See Appendix B for further details of input data for the seabed characteristics used for clay and sand. The legs are rigidly fixed to the hull during the course of one simulation. However, in reality leg length continuously increases. Therefore, several simulations are carried out with the tip of the spudcan at different initial distances from the mudline for each seastate as captures of single time instants of the jacking procedure. Thus, the initial distance to mudline is varied from 0 m to -1.2 m, for sand, and 0 m to -1.5 m, for clay, in steps of 0.3 m totalling five simulations for sand and six simulations for clay to be carried out for each seastate. For rock, only one simulation is performed at an initial distance to mudline at 0 m. Negative values correspond to depths below the mudline.

Time-series containing vessel motion in 6 DOFs and translational forces on the spudcans are an output from the time-domain simulations. In the time series for the translational forces, only the time steps where the spudcan is actually moving downwards are extracted, in accordance with the definition of impact presented in Section 2.

5.2 FE simulation procedure

The aim of the FE simulation is to study the capacity of the structure. The structural capacity is seen as the maximum load the structure can carry. When the load exceeds the capacity it fails, and failure is defined using the structural evaluation criteria. An evaluation of the structural capacity can be done in numerous different ways. The choice of method is dependent on the acquired level of accuracy in the results. The capacities in this thesis are calculated using FE simulations and the capacity is presented as a failure surface. A failure surface can be used for describing the change in structural capacity towards loads in different directions but with the same point of attack. The failure surface is defined by a database of simulations that are made by applying an increasing load on the structure and evaluating when the structure fails in terms of the structural evaluation criteria. The procedure is repeated for a sufficient

numbers of load cases and the structural capacity is then described by a piecewise linear failure surface.

5.2.1 Structural evaluation criteria

The structural capacity can be evaluated using different kinds of criteria and modes of failure. DNV (2012) states that for the structural design it is necessary to evaluate the designed resistance against the following failure modes:

- Excessive yielding
- Buckling
- Brittle fracture
- Fatigue fracture

Fracture due to fatigue is not a part of this thesis and since brittle fracture is not normally considered in structural design and dependent on selection of material (DNV, 2012), it is not considered in this report. Hence, only yielding and buckling is part of the analysis and are further on referred to as evaluation criteria.

The von Mises yield criterion is used for evaluating the stress state in the material and thus determining whether a material experience stresses above or below the yield strength. In general terms, the von Mises yield criterion is described by:

$$\sigma_{vM} = \sqrt{\frac{1}{2}[(\sigma_{11} - \sigma_{22})^2 + (\sigma_{22} - \sigma_{33})^2 + (\sigma_{33} - \sigma_{11})^2 + 6(\sigma_{12}^2 + \sigma_{23}^2 + \sigma_{31}^2)]} \quad (5.1)$$

Buckling is an instability phenomenon that is a result from high compressive stresses in a structural member. The phenomenon is characterized by a sudden failure, where the compressive stresses at the point of failure are less than the ultimate strength of the material. Buckling may occur both as a fully elastic phenomenon or a plastic phenomenon. For example, the well-known formulas for buckling of columns presented by Euler are valid for purely elastic deformations, i.e. the columns will regain their initial shapes when unloaded. The structure is evaluated against elastic buckling failure using the BUCKLE solver in ABAQUS, which solves an eigenvalue problem out of which the three smallest eigenvalues are extracted. Critical buckling loads and buckling modes are assessed using the results from the FE simulation in a methodology presented by DNV (2004). The methodology is based on the reduced slenderness of the structural members defined as:

$$\lambda = \sqrt{\frac{\sigma_y}{\sigma_E}} \quad (5.2)$$

σ_y is the yield strength of the material and σ_E is the critical elastic buckling stress achieved from the FE simulation. Cross-section-dependent parameters needed for calculating the critical buckling stress are presented in Table 5.1.

Table 5.1 Cross-section-dependent parameters used for calculating critical buckling stress.

<i>Cross-section-dependent parameters</i>	α	λ_0	μ
Tubular members (leg)	0.2	0.2	$\alpha(\lambda - \lambda_0)$
T-sections (stiffeners in spudcan)	0.5	0.2	

The critical buckling stress can then be calculated using the following expressions:

If $\lambda \leq \lambda_0$

$$\sigma_{cr} = \sigma_F \quad (5.3)$$

If $\lambda > \lambda_0$

$$\sigma_{cr} = \sigma_F * \frac{1 + \mu + \lambda^2 - \sqrt{(1 + \mu + \lambda^2)^2 - 4\lambda^2}}{2\lambda^2} \quad (5.4)$$

The critical buckling modes are in this method calculated using the fraction between the yield stress in the material and the critical elastic stress simulated using FE. However, the FE simulations give the critical elastic buckling force that needs to be translated into stresses. Assuming that the force-stress relation is linear it is possible to derive a correlation between the applied force (impact load) and the stress in the element where the critical buckling occurs. Using the correlation it is possible to find the critical buckling stress for the critical buckling force.

5.2.2 Loads and boundary conditions

The motion of the vessel that dominates during the impact scenario is the rotational degrees of freedom roll and pitch (DNV, 2012). This means that the force acting on the spudcan during the impact will have a vertical and a horizontal component in a loading plane. To account for this in the capacity evaluation, different load directions with the same point of attack have been considered. This is done for the three wave headings considered. The load directions considered are described by vectors where (x,y,z) correspond to the coordinate system presented in Figure 3.5. The vectors are presented as three dimensional but lie in three different planes, i.e. the loading planes according to Figure 3.2:

$$\mathbf{F}_{90^\circ} = \begin{bmatrix} F_X \\ F_Y \\ F_Z \end{bmatrix} = \begin{bmatrix} 0 & 0 & 0 & 0 & 0 & 0 & 0 & 0 & 0 \\ 1 & 1 & 1 & 1 & 1 & 1 & 1 & 1 & 1 \\ 0 & 1 & 2 & 4 & 6 & 10 & 15 & 20 & 1 \end{bmatrix} MN \quad (5.5)$$

$$\mathbf{F}_{135^\circ} = \begin{bmatrix} F_X \\ F_Y \\ F_Z \end{bmatrix} = \begin{bmatrix} \frac{1}{\sqrt{2}} & \frac{1}{\sqrt{2}} \\ \frac{1}{\sqrt{2}} & \frac{1}{\sqrt{2}} \\ 0 & 1 & 2 & 4 & 6 & 10 & 15 & 20 & 1 \end{bmatrix} MN \quad (5.6)$$

$$\mathbf{F}_{180^\circ} = \begin{bmatrix} F_X \\ F_Y \\ F_Z \end{bmatrix} = \begin{bmatrix} 1 & 1 & 1 & 1 & 1 & 1 & 1 & 1 & 0 \\ 0 & 0 & 0 & 0 & 0 & 0 & 0 & 0 & 0 \\ 0 & 1 & 2 & 4 & 6 & 10 & 15 & 20 & 1 \end{bmatrix} MN \quad (5.7)$$

The loads used in the capacity evaluation are applied quasi-statically on the structure meaning that any dynamic effects are disregarded. No dynamic amplification factor has been used to compensate for this. The loads are then increased in step of 1 MN and stopped when failure due to the assessment criteria occurs. The simulations are repeated for each criteria. The mesh convergence study showed that there will be critical regions in the spudcan, which means that the load application area affects the capacity of the structure. The critical region of the spudcan is in the top plate and that response is dependent on the distribution of the load. Loads far from the leg govern bending stresses where it is attached to the spudcan due to bending. See Figure 5.2. The conservative approach, resulting in the lowest capacity, is therefore to apply the load on the entire bottom plate, which will be done in all further simulations. The load is applied as a volume load in the FE simulations to be able to freely choose loading direction. The volume of the bottom plate is used as reference for the volume load

application. Furthermore, the leg is modelled as rigidly fixed to the hull as the stiffness of the hull is relatively large compared to the stiffness of the legs (Williams et al., 1997).

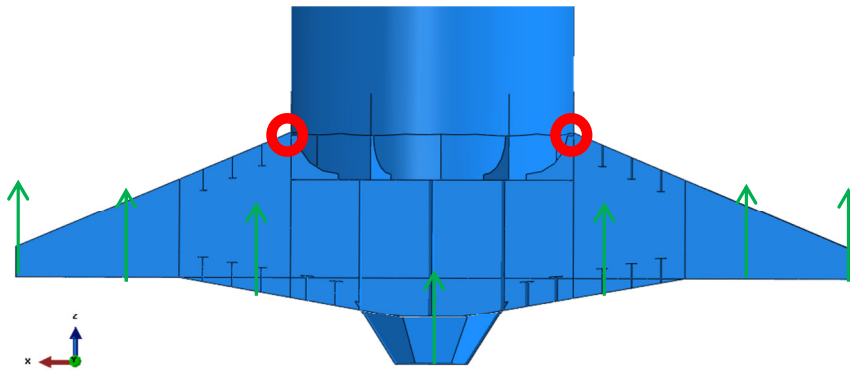


Figure 5.2 The load applications are shown with green arrows. The critical region concerning stresses is marked with red circles.

6 Results

This section presents and discusses the results from the case study. The section is divided into three subsections, dedicated to describing the results from the time-domain simulations, the FE simulations and the combined results for the structural utilization grade for the obtained impact loads.

The concept of a loading plane as presented in Section 3 is shown in more detail in Figure 6.1. The horizontal and vertical forces in Figure 6.1 are acting on the spudcan and the force vector can also be defined by magnitude and angular deviation from the vertical axis. The origin of the coordinate system used in Figure 6.1 is located so that it coincides with the point of attack of the loading. The dashed black line represents an imaginary capacity against forces acting in the origin. The force magnitude is evaluated against the capacity utilizing a usage factor defined as:

$$UF = \frac{\text{Impact force}}{\text{Capacity}} = \frac{F_{\text{impact}}}{F_{\text{cr}}} \quad (6.1)$$

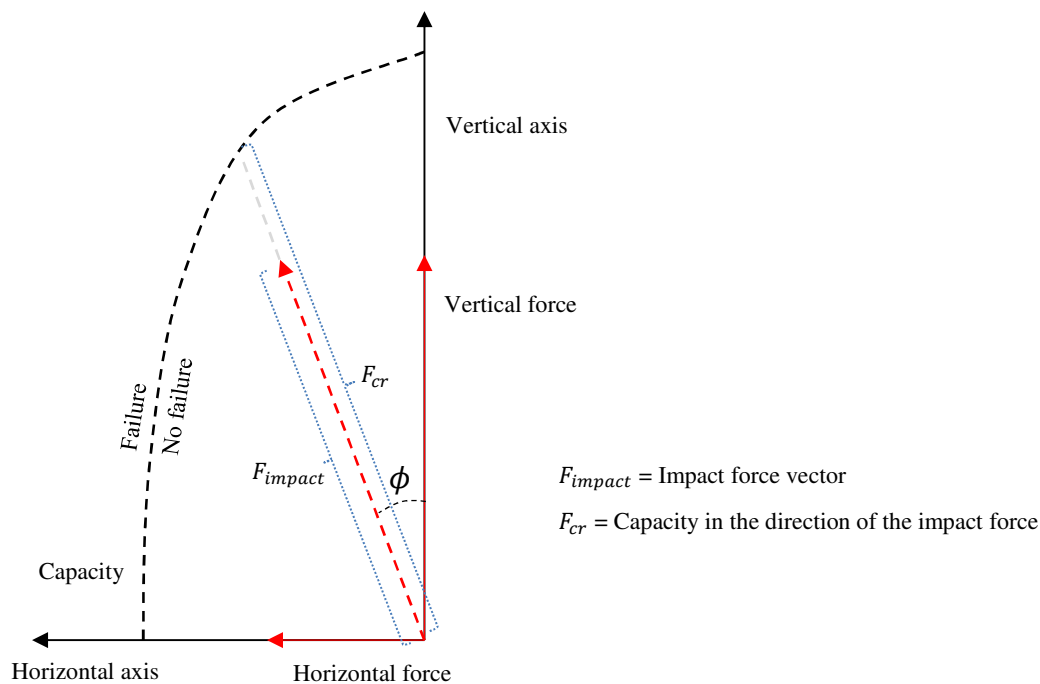


Figure 6.1 Detailed schematic diagram of a loading plane and how the loads and capacity are defined using this plane. The point of attack of the forces is the spudcan bottom plate, coinciding with the origin of the coordinate system, with the vertical axis extending upwards along the leg.

6.1 Impact forces

Magnitudes are used to describe the forces in the report. This is motivated by large vertical forces in comparison with horizontal forces. Thus, the direction of the forces does not deviate in excess of approximately 5 degrees from the vertical axis, see Figure 6.1. Impact force magnitudes obtained from time-domain simulations are shown in Figure 6.2. Each plot, one for each combination of wave period (T_p) and wave heading, shows impact force magnitude as a function of significant wave height (H_s) for three different seabed characteristics. Additionally, impact force magnitudes

calculated by DNV's recommended practice are presented in the plots for headings of 90 degrees and 180 degrees but are omitted for 135 degrees as the formulas do not cover this. The magnitudes in Figure 6.2 are the largest observed magnitudes over the simulation length, 3,600 s, for each seastate. As such, the magnitudes of the forces are not necessarily representative for the seastate from which they are extracted but the plots in Figure 6.2 should rather be considered as a way of visualizing trends and comparing forces obtained with different seabed characteristics. One extreme seastate ($H_s = 7 \text{ m}$, $T_p = 12 \text{ s}$) was also simulated in the time domain and the impact force magnitudes obtained from these simulations are presented in Table 6.1.

Some RAOs for the vessel used for the case study may be found in Appendix A. The results presented in Figure 6.2 will partly be discussed using these as a base. Generally, the impact forces increase when the incoming waves move from head seas (180 degrees) to beam seas (90 degrees). This is to be expected as vessels in general, also the one described here, are more sensitive to disturbances from waves in the transverse direction. In almost all of the plots, it is also clearly visible that impact force magnitudes increase with increasing wave height, which is also to be expected based only on the RAOs for the vessel. For some of the shortest wave periods, however, this is not always the case. This is believed to originate from the very small motions of the vessel for these periods, as that in turn makes the model more sensitive to other disturbances such as numerical errors, etc. The magnitudes of the measured impact forces increase quite rapidly as the wave periods are increased from their lowest value. However, the forces do not continue to increase as the wave period continues to increase. Remembering that the eigenperiods of the vessel lie around 8-11 seconds, these results are indeed to be expected and if simulations had been run for even larger wave periods, a slight decrease of impact force magnitudes would have been plausible.

The magnitudes calculated by DNV's recommended practice are larger than the magnitudes obtained from the impact model presented in this thesis in all cases but for the shortest wave period. This is also valid for the magnitudes obtained when using rock as a seabed, even though the magnitudes obtained from these simulations do not always deviate that much from the magnitudes obtained by the DNV approach. Nonetheless, these results ratify the belief that the approach used by DNV gives conservative estimates.

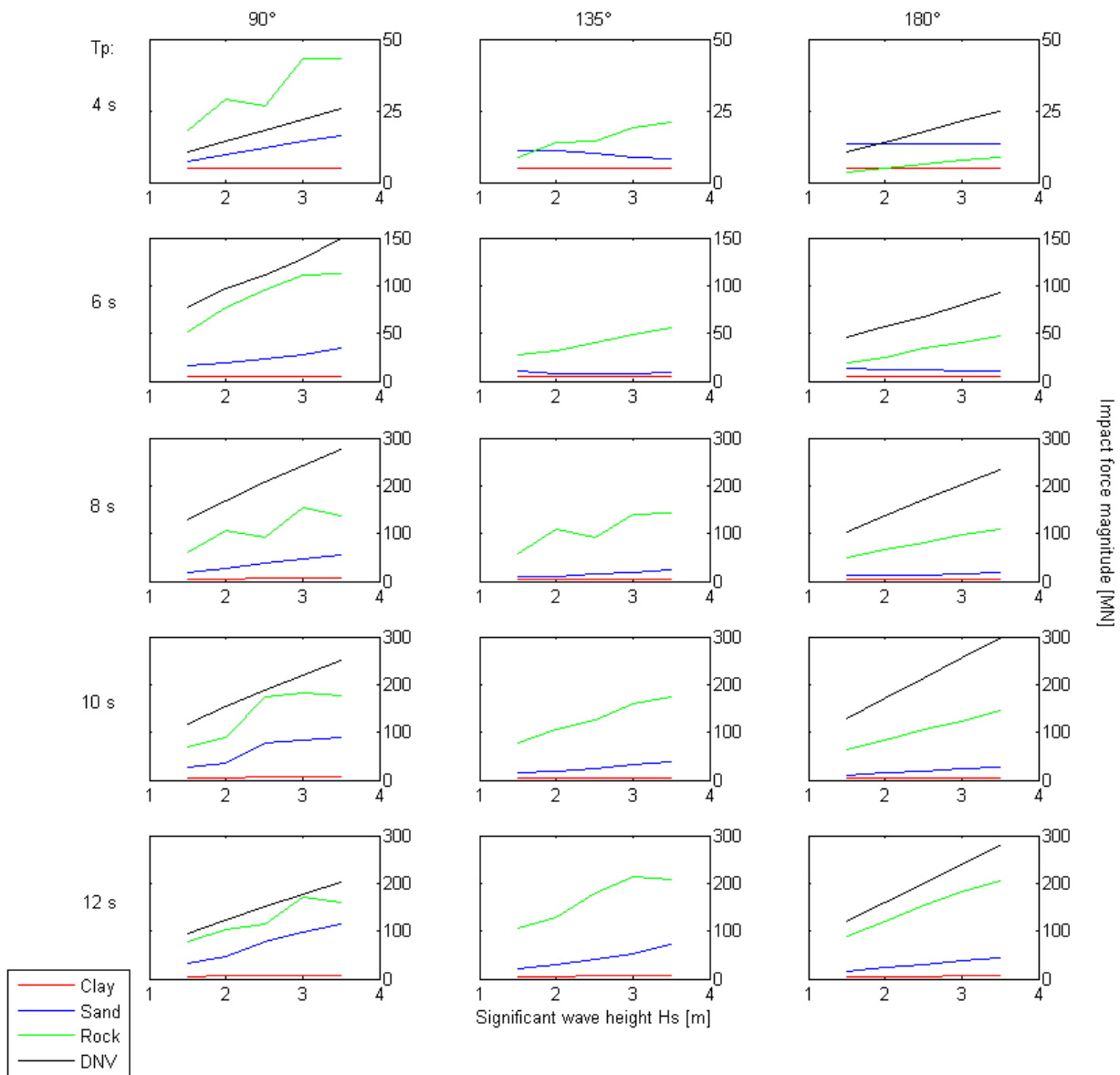


Figure 6.2 Impact force magnitudes [MN] for three different seabed characteristics plus magnitudes calculated by DNV's recommended practice as a function of significant wave height (H_s) for each combination of wave period (T_p) and wave heading.

Table 6.1 Impact force magnitudes [MN] for extreme seastate ($H_s = 7$ m, $T_p = 12$ s).

Heading	Clay	Sand	Rock	DNV
90 degrees	17.2	145.4	324.7	356.2
135 degrees	10.5	139.2	417.5	
180 degrees	9.6	137.8	391.1	568.3

All the results presented in Figure 6.2 are based on the largest observed impact force magnitude for simulations of a length of 3,600 s and these results are not necessarily representative for the seastate from which they are obtained. A small study of the degree of fluctuation of the magnitudes for a single seastate and a single soil type has been conducted in order to put the results presented in Figure 6.2 in perspective. Figure 6.3 shows observations of the largest impact force magnitude for 15 different realizations (seed numbers) of the same seastate ($H_s = 2\text{ m}$, $T_p = 6\text{ s}$) for a sandy seabed ($\phi = 35\text{ degrees}$). Note that seed nr. 1 corresponds to the realization used for the results presented in Figure 6.2. The mean of the observations is 19.3 MN and the observations range from 16.8 to 22.5 MN. The standard deviation from the mean is 1.6 MN.

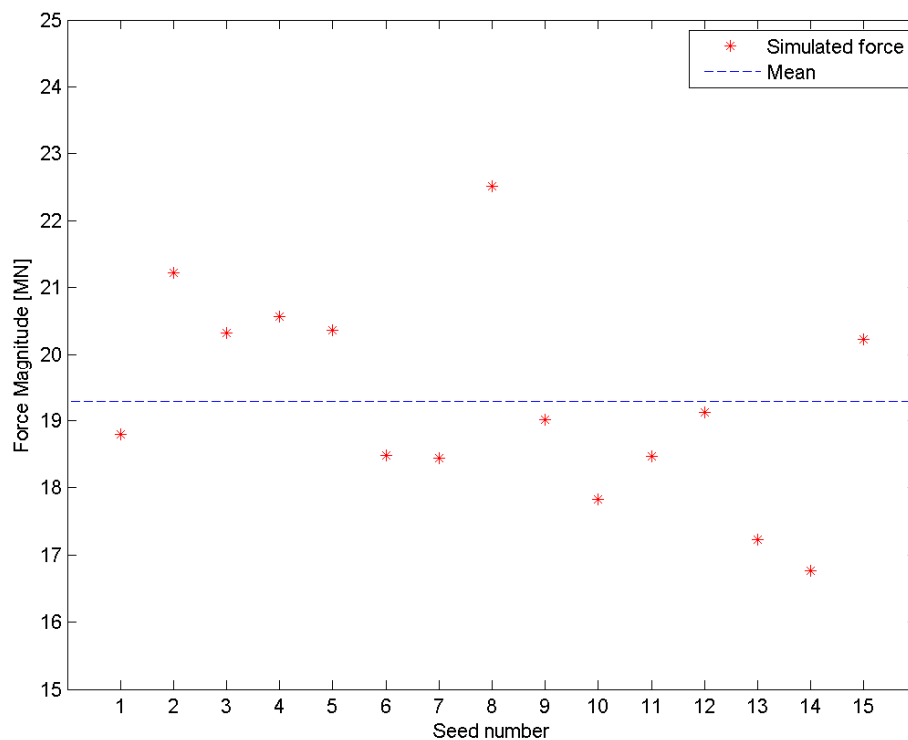


Figure 6.3 Observations of the largest impact force magnitude for 15 different realizations (seed numbers) of the same seastate ($H_s = 2\text{ m}$, $T_p = 6\text{ s}$) for a sandy seabed.

6.2 Structural capacity

The structural capacity is evaluated using a series of FE simulations that are done in order to describe strength of the structure against the structural evaluation criteria yielding and buckling. The FE simulations are performed by applying loads on the bottom plate of the spudcan with different angles of attack and establishing the critical magnitude for the angle of attack with regards to the evaluation criteria, see Section 5.2.1. The results of these simulations are described using a failure surface, plotted on the loading planes corresponding to the wave heading analysed. These failure curves are presented in Figure 6.4 followed by descriptions of the critical failure modes.

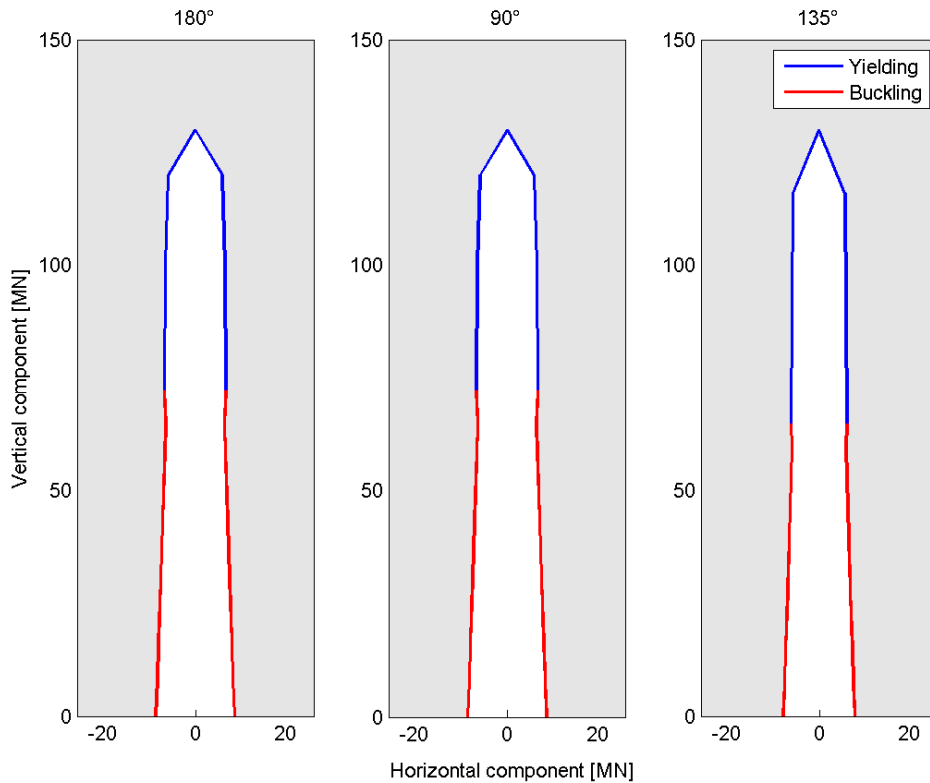


Figure 6.4 The failure surface for the leg/spudcan-structure shown in the three loading planes corresponding to the wave heading considered in the thesis. Loads acting on the structure have their point of attack in the origin of the coordinate system. Subsequently, loads reaching out into the grey area correspond to failure according to the structural evaluation criteria and loads housed in the white area are within the limits for the structural evaluation criteria.

The failure surface is defined by two different failure modes. The blue line corresponds to yielding in the top plate of the spudcan due to vertical loads and the red line corresponds to local buckling in the edge of the top holes in the leg. Both modes are explained more thoroughly below.

Horizontal forces on the spudcan generate a bending moment in the structure as the top of the leg is modelled as being fixed to the hull. The bending moment is dependent on the lever, which in this case means the length of the leg as the load and the fixed support is on each side of the leg. The stresses due to the bending moment should therefore appear in the top rim of the leg. However, the leg is pierced with holes that generate stress concentrations. These compressive stresses will cause a local buckling that is shown in Figure 6.5. In the case with a uniaxial horizontal load this failure mode corresponds to $\mathbf{F}_{cr} = \begin{bmatrix} 8.7 \\ 0 \\ 0 \end{bmatrix} MN$ or $\mathbf{F}_{cr} = \begin{bmatrix} 0 \\ 8.7 \\ 0 \end{bmatrix} MN$ (due to symmetry in the leg).

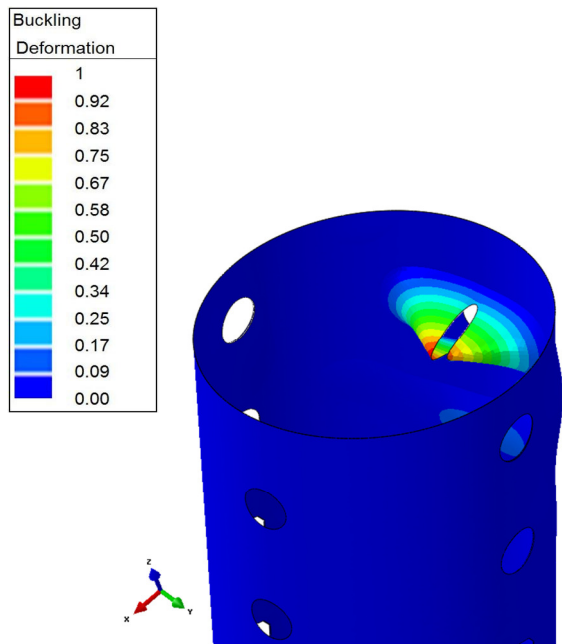


Figure 6.5 The top holes of the leg are the critical region with regard to buckling for horizontal loads acting on the bottom plate in head seas (x -dir). Due to symmetry in the leg, the buckling mode will look identical for horizontal loads in beam seas (y -dir). The failure mode is simulated using a unit load, the deformation is therefore not connected to the critical load and the contour plot only visualizes the buckling shape.

For the case with waves approaching from 135 degrees the buckling mode looks slightly different, see Figure 6.6, and corresponds to $\mathbf{F}_{cr} = \begin{bmatrix} 5.73 \\ 5.73 \\ 0 \end{bmatrix} MN$.

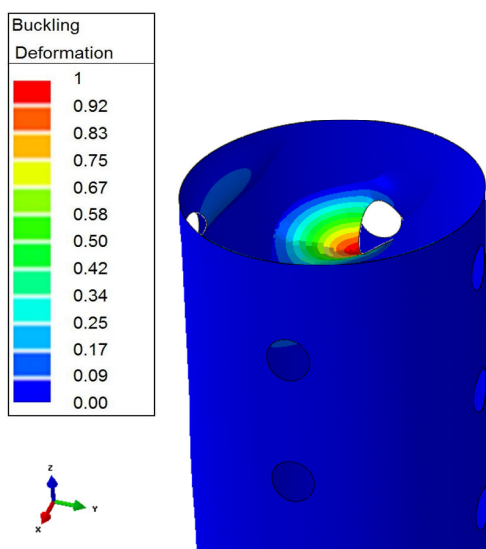


Figure 6.6 The top holes of the leg are the critical region with regard to buckling for horizontal loads acting on the bottom plate in quartering sea. The failure mode is simulated using a unit load; the deformation is therefore not connected to the critical load and the contour plot only visualizes the buckling shape.

When the bottom plate is instead subjected to vertical loads the critical regions of the structure is in the top plate of the spudcan. As the load is distributed evenly over the entire bottom plate the top plate of the spudcan will be subjected to compressive loads. As the leg creates a hole in the top plate stress concentrations will rise, as can be seen in Figure 6.7. The top of the spudcan can be seen as a plate with a circular hole loaded in-plane in two directions. The highest stresses will then arise obliquely between the loading directions, as can be seen in Figure 6.7. The critical force for yielding in the case with a pure vertical load is $F_{cr} = \begin{bmatrix} 0 \\ 0 \\ 130 \end{bmatrix} MN$.

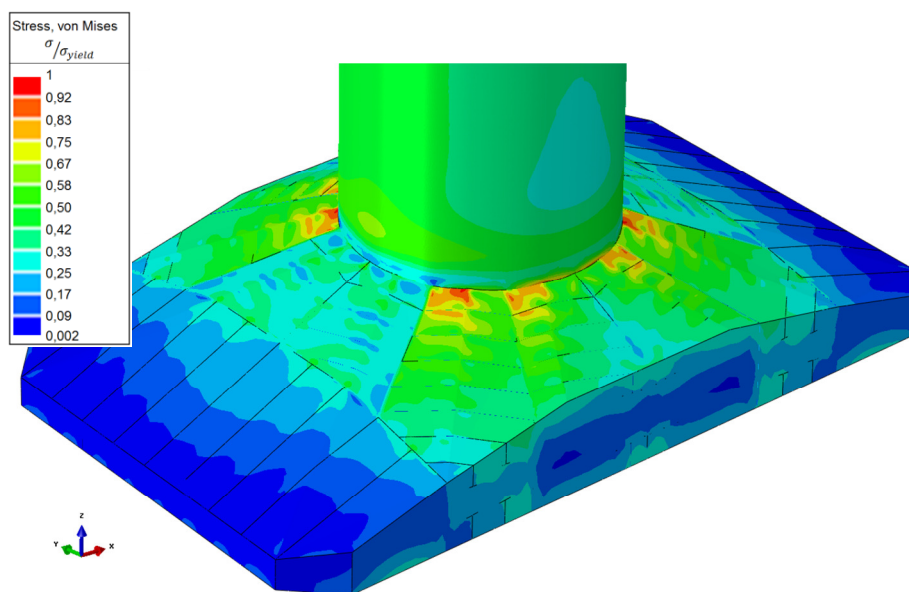


Figure 6.7 The top plate of the spudcan is the critical region with regard to yielding for vertical loads acting on the bottom plate.

As the load direction moves from the purely horizontal towards the vertical case the critical mode changes. The point when the critical failure mode switches from local buckling in the leg to yielding in the spudcan top plate is highly dependent on the level of discretization. The number of simulations used in this case study is presented in Equation 5.5-7. The entire structural analysis with more failure modes can be found in Appendix C.

Note that the structural capacity against failure as presented in Figure 6.4 only accounts for the analysed leg and spudcan. The leg of the vessel is attached to the hull through a jackhouse where the jacking mechanism supports and elevates the leg. The jackhouse is modelled as a fixed boundary in the model as the stiffness of the hull is thought to be much larger than the stiffness of the analysed structure. However, the structural strength of components in the jackhouse is not assessed and any failure there is unaccounted for. The operational static holding capacity of the ship is 9,000 tonnes, but in this mode the leg is locked and not elevating. The operation discussed in this thesis is when the elevating and the corresponding limit is the jacking capacity, 5300 tonnes. The limit corresponds to almost 53 MN and should be interpreted as an operational limit and not be compared with the structural capacity evaluated in this thesis without considering appropriate safety margins. However, as it lies well under the simulated structural capacity and in the same range as some of the simulated impact loads it is a factor that could possibly be limiting.

6.3 Weather window

The UF relates the loads on the structure with its capacity against failure in the direction of the loading, see Figure 6.4, and thus giving an estimate about to what extent the structural capacity is utilized. A UF equal to one thus corresponds to the point where the structure fails. Usage factors for the simulated seastates are presented in Table 6.2 for sand, Table 6.3 for rock and Table 6.4 for DNV recommended practice. Impact in clay generates very small impact forces, see Section 6.1, and consequently the structural utilization grade is small and will not be shown here. The extreme seastate produces a UF factor equal to approximately 13%, whereas the worst “regular” seastate produces a UF factor equal to approximately 7%. Note that no safety margins are implemented in these results. The latter also means that no operational limits can be interpreted directly from these results. Trends obviously follow the same pattern as for the impact forces, see Section 6.1, and will not be discussed here more thoroughly than is done below.

In sand, the structural capacity is exceeded only for the extreme seastate and by only a few percent. It is also clearly visible that beam sea is the most strenuous condition of the three rendering the largest usage factor in almost all seastates. Rock is generally worse than both clay and sand, rendering quite large usage factors even for the smaller seastates. Interestingly enough, quartering seas seem to be the most strenuous condition for larger seastates, whereas beam seas produce the largest usage factors for the smaller seastates. The comparative calculations made with the recommended practice by DNV (2012) produce the largest usage factors for all seastates except for the ones with the shortest wave period in beam seas. For DNV recommended practice, head sea turns out to be the most strenuous condition.

In general, it seems like the most strenuous incoming wave direction changes from beams seas for softer seabeds to quartering and head seas for harder seabeds. It is, however, difficult to speculate about the reason for this behaviour. It could be due to difference in movement pattern of the vessel because of previous impacts in harder seabeds having a large influence. Also, it is quite evident that the utilization grade differs greatly with type of seabed and that approximating the seabed as infinitely rigid as done by DNV, see Section 2, does produce a great estimate of impact forces.

Table 6.2 Usage factors for simulated impact forces in sand.

Sand $\phi = 35$ degrees		H_s [m]					
Heading	T_p [s]	1.5	2	2.5	3	3.5	7
180 degrees	4	0.10	0.10	0.10	0.10	0.10	
	6	0.10	0.10	0.09	0.09	0.08	
	8	0.09	0.09	0.10	0.12	0.14	
	10	0.08	0.12	0.15	0.18	0.21	
	12	0.13	0.18	0.23	0.29	0.35	1.06
135 degrees	4	0.09	0.08	0.08	0.07	0.07	
	6	0.08	0.07	0.06	0.06	0.07	
	8	0.08	0.09	0.12	0.14	0.19	
	10	0.11	0.15	0.18	0.25	0.30	
	12	0.17	0.24	0.31	0.40	0.55	1.07
90 degrees	4	0.06	0.07	0.09	0.11	0.13	
	6	0.12	0.15	0.18	0.21	0.26	
	8	0.14	0.22	0.30	0.36	0.42	
	10	0.20	0.27	0.60	0.65	0.69	
	12	0.24	0.35	0.59	0.75	0.89	1.12

Table 6.3 Usage factors for simulated impact forces on rock.

Rock		H_s [m]					
Heading	T_p [s]	1.5	2	2.5	3	3.5	7
180 degrees	4	0.03	0.04	0.05	0.06	0.07	
	6	0.14	0.19	0.27	0.31	0.36	
	8	0.38	0.51	0.63	0.75	0.84	
	10	0.50	0.64	0.81	0.95	1.12	
	12	0.69	0.93	1.18	1.41	1.58	2.50
135 degrees	4	0.07	0.11	0.11	0.15	0.16	
	6	0.22	0.24	0.31	0.38	0.43	
	8	0.46	0.84	0.72	1.07	1.09	
	10	0.60	0.82	0.97	1.23	1.33	
	12	0.82	1.00	1.39	1.63	1.61	3.21
90 degrees	4	0.14	0.22	0.21	0.33	0.33	
	6	0.39	0.60	0.73	0.86	0.87	
	8	0.47	0.83	0.71	1.19	1.07	
	10	0.54	0.68	1.33	1.41	1.35	
	12	0.59	0.80	0.88	1.32	1.24	2.50

Table 6.4 Usage factors for impact forces according to DNV. The recommended practice does not support combination of pitch and roll which is why quartering seas (135 degrees) is omitted.

DNV		H_s [m]					
Heading	T_p [s]	1.5	2	2.5	3	3.5	7
180 degrees	4	0.08	0.11	0.14	0.17	0.19	
	6	0.36	0.45	0.52	0.62	0.72	
	8	0.81	1.08	1.35	1.59	1.81	
	10	1.00	1.33	1.66	1.99	2.32	
	12	0.93	1.24	1.55	1.86	2.17	4.44
90 degrees	4	0.08	0.11	0.15	0.18	0.21	
	6	0.61	0.77	0.88	1.02	1.18	
	8	1.03	1.35	1.66	1.94	2.20	
	10	0.94	1.22	1.49	1.75	2.01	
	12	0.75	0.98	1.20	1.40	1.60	2.84

7 Discussion

This section discusses the proposed methodology of analysis and the software implementation from a broader perspective. The results obtained from the case study will not be treated explicitly in this section. Some of the sources of error introduced by the chosen simulation techniques as well as some of the simplifications made in the models will also be discussed.

Simulation approach

Using time-domain simulations to evaluate impact forces is just one of several possible approaches. A frequency-domain analysis of the vessel motions is another. Frequency-domain analyses make use of a linear theory enabling shorter computation times than time-domain analyses. The advantages of time-domain analyses over frequency-domain analyses lie within the ability to capture non-linear phenomena such as interaction with the seabed allowing coupled simulations to be performed, which is the reason for using it in this thesis. Using a frequency-domain analysis would imply that the hydrodynamic and soil impact analysis would have to be uncoupled.

FE simulations are also just one way of evaluating structural capacity. Analytical beam theory gives very good estimates of the structural capacity of the leg, see Section 4.2, and is a very useful tool for simpler geometries. However, for assessing the complex geometry in the spudcan it is not an efficient tool. FE simulations on the other hand introduce numerical uncertainties derived from, for example, convergence issues and skewed elements and also increase the complexity of the analysis method quite extensively. The analyses of the loads and the capacity against the loading are uncoupled, i.e. the FE analysis is not directly coupled to the time-domain analysis. This approach is chosen in order to avoid complex software interactions and maintain manageable computation times. A less complex structural evaluation analysis methodology could be implemented, thus lowering the computation time requirements. This could be an interesting evolution of the methodology as dynamic structure interaction can be directly incorporated.

The simulation methodology as such is directly applicable on a case study involving, for example, another vessel and other soil types whereas changes to the submodels are necessary. Other soil types result in relatively minor changes whereas another vessel requires some more extensive alterations in the submodels. The evaluation criteria used in this work is quite easily exchanged due to the uncoupled nature of the simulations. The coupled time-domain simulation methodology is primarily developed for the type of impact scenario discussed in this thesis, but is believed to be applicable also to other similar scenarios where soil-structure interaction is present. One example is installation of pile foundations for bottom-fixed wind turbines with a hydraulic hammer.

Evaluation criterion

The weather window assessments are made comparing impact forces from the time-domain against the capacity of the structure evaluated using FE simulations. As such, the evaluation criterion is purely structural. However, it is believed that other evaluation criteria could be equally important to address. For example, the ship has a big deck with sea-fastened equipment and cargo that could be sensitive to accelerations in an impact scenario. The evaluation criteria being the foundation for

the usage factor calculation are in this thesis defined using the structural capacity defined by only yielding and buckling. The entire structural integrity is hence not accounted for, as failure due to fatigue and fracture is disregarded. The impact scenario governs relatively high loads and in an operational pattern where the ship operates in a harsh environment with frequent installation and retrieval it would be of great interest to study the fatigue response. Also, the structure is expected to function in a harsh, corrosive and occasionally cold environment increasing its vulnerability.

When comparing the impact loads simulated in the time domain simulations with the structural capacity through the UF-factor it is important to realize that it is the limit for failure that is assessed. Any attempt on conclusions about an operational limit must be preceded by a safety margin implementation and preferably a statistical verification of the results.

Definitions

In this thesis, impacts are defined as the time interval when the spudcan of the SEU penetrates the seabed vertically. However, it has been noted that during these time-intervals, horizontal forces are almost non-existent, both in sand and clay, as the course of action is dominated by vertical motion. Studying the time-series for both clay and sand, it turns out that horizontal forces are indeed very small during the time interval of an impact, but has a maximum just after the vertical penetration has ended. This implies that the structural loading is actually a loading in two phases: one initial impact phase, as has been studied in this thesis, dominated by vertical force and one following phase where the horizontal force has its maximum and the vertical force is rather small. This phenomenon should be much more pronounced for impacts in clay as the horizontal capacity is depth-dependent. For sands, where the horizontal capacity is dependent on the actual vertical force, sliding of the spudcan is a more likely result than large horizontal forces.

Limitations and simplification in time-domain analyses

Impacts are studied as a phenomenon caused by waves. However, other environmental forces originating from, for example, wind or current can also affect the vessel motion on location and consequently affect the impact scenario even though it is believed that waves are the major contributing factor. The water depth is also believed to have an effect on the impact forces as it affects the spudcan motion both directly, in terms of geometry, and indirectly in terms of changing hydrodynamic properties of the vessel with changing leg length. However, the choice of keeping the water depth fixed in the case study is a conscious one to in order to maintain a focus on the performance of the impact model and the soil-structure interaction.

The impact forces from the time-domain simulations are obtained using several simplifications. First off, the seabed is assumed to be homogenous. This is rarely the case in reality. However, bearing in mind that penetration only exceeds 1.5 m in the case of clay, which does not give impact forces anywhere near the structural capacity, it is reasonable to believe that the first 1.5 m or so of the seabed may be approximated as homogenous. The theoretical framework used for describing soil deformation behaviour only accounts for permanent (plastic) deformation. Omitting the small elastic part of the soil behaviour is not believed to have a large effect on the impact forces as such, but as this is the main difference between bearing capacity and cavity expansion theory it should be a topic for further investigation. Additionally, neither the bearing capacity theory in general nor the implementation in SIMO account for the load history of a soil meaning that every simulated impact is conducted to

untouched soil even though unrecoverable plastic deformation, with possible plasticity hardening effects, occur for every impact. This produces smaller force estimates for soils where plastic deformation is expected, such as in clay or sand.

Simulation of the vessel motion is conducted assuming a rigid hull motion. This is an often made and generally accepted assumption of motion in waves as hulls are generally comparatively stiff and the elastic deformations are small. However, during impact to the seabed the hull most probably cannot be assumed to behave as a stiff body as the stiffness of both the seabed and the leg (in the axial direction) can be comparatively very stiff. Hydrodynamic properties such as added mass and drag coefficients of legs and spudcans also affect the vessel motion. Even though the proximity to the seabed is apparent, the hydrodynamic properties have not been adjusted for this. However, it is not believed to have a great effect on the vessel motion as they are relatively small in any case.

The horizontal anchor system of the hull may also have an influence, perhaps affecting the roll or pitch motion, on the obtained impact forces. However, a similar phenomenon exists in reality where the DP-system of the vessel affects the motion of the vessel and thus also the impact forces. The similarity or dissimilarity of the effects from a horizontal anchor system and a DP-system is, however, outside the scope of this thesis and is neglected as a minor influence on the impact forces. To perform simulations in the time-domain for several time instants of the jacking procedure with the spudcans at different positions instead of simulating the whole procedure with a continuous lowering of the legs has both advantages and disadvantages. By not performing simulations for the whole jacking procedure, there is obviously a risk of omitting sequences of the procedure which one might not consider to be critical but where the results show otherwise. On the other hand, for the time instants chosen during the jacking procedure, it is possible to perform as long simulations as are deemed necessary and for different realizations of the same seastate.

The vessel has four spudcans, each one of them making contact with the seabed during a simulation. In the post-processing of the data the time-series of impact forces acting on the four spudcans are concatenated and analysed as a single time-series. As such, information about which spudcan suffers the largest impact during a simulation is not stored. This does not affect the result presented in this thesis but the information might be valuable if investigations of other aspects are conducted.

Limitations and simplifications in FE analyses

The FE analysis is performed on a model consisting of one leg and one spudcan off the type used on the case vessel. The loads acting on the FE model are distributed evenly on the entire bottom plate of the spudcan. This is a simplification, as the impact loads in reality will propagate over the conical bottom plate and be dependent on penetration depth. This assumption is valid for softer soils such as clay and sand but is not as accurate in cases with harder seabeds consisting of rock. Nonetheless, applying the loads on the full bottom plating is the conservative approach as the capacity has a minimum for this load application. Furthermore, the loads are applied quasi-statically meaning that no dynamic effects are considered in the results for the structural capacity. The impact forces from the time-domain are obtained accounting for some dynamic effects such as inertia. Strain-rate hardening effects of the structure are, however, not accounted for meaning that the forces could be underestimated. When assessing the structural capacity, no dynamic effects are accounted for at all. Inertia effects are believed to be rather small, especially in the vertical direction where

the structural stiffness is very high. Effects originating from the high strain-rate, however, are believed to affect the structural capacity as not only material parameters such as stiffness is influenced but also parameters such as material strength. To include strain-rate effects in the methodology is thus of interest.

The connection between leg and hull is modelled as a fixed boundary condition meaning that no deformation from the impact energy is absorbed in the hull. This could affect the structural capacity as the elasticity connected with this boundary is not accounted for. It also means that the strength of the jackhouse and the jacking system is disregarded in the evaluations. Assessing the structural strength of jackhouse and jacking system is of great interest as it could be a critical criterion in assessing the weather window. There are no considerations regarding welds in the FE model. Welds usually govern residual stresses from the manufacturing that needs to be considered. There are two critical failure modes presented in Section 6.2: a buckling mode in the leg governed by horizontal loads according to Figure 6.5-6 and one yield failure governed by vertical loads according to Figure 6.7. The buckling mode in the leg is in a region free from welds meaning that the assumption to disregard it is valid. However, in the vertical load case the failure mode is in a region where the leg is attached to the spudcan. This region has a lot of welds and residual stresses could be substantial. How this effects the structural capacity is not studied in this thesis.

The loads and thus also the structural capacity is simplified to two dimensions where the transverse (relative to incoming waves) force component in the horizontal plane is disregarded. The disregarded component is not believed to have and influence on the results presented in this thesis, as the magnitudes are comparatively small and thus do not come in the vicinity of the structural capacity. However, they could prove important in a fatigue assessment where even loads of rather small magnitudes affect the life of the structure.

8 Conclusions

The objective of this thesis has been to develop a method of analysis by which it will be possible to make weather window assessments for the installation and retrieval phases of a SEU. The method of analysis will take site-specific parameters, defined as soil type and water depth, into account in addition to vessel-specific and environmental parameters. The inclusion of site-specific parameters is the novel contribution compared to assessment methodologies used today. The method of analysis is to include the possibility of making assessments using different evaluation criteria, while the assessments in this thesis are limited to a structural evaluation criterion. The method of analysis is to be tested and evaluated. Using the developed method of analysis, a study will be conducted with the aim of learning more of the physics behind and the sequence of events during an impact as well as investigating the necessity of including site-specific parameters in such assessments altogether.

A theoretical impact model capable of describing the soil-structure interaction between seabed and spudcan during impact has been found through a literature study of existing impact theories and soil penetration theories. The theoretical model is a combination of two existing theories applied in series with each other to describe the behaviour of both the structure and the soil during impact. The soil model is based on the bearing capacity theory and the structural model is based on contact mechanics, i.e. a spring and damper system. The full theoretical model is able to describe the vertical and horizontal forces arising on the spudcan during an impact, but is limited to plastic deformation of the soil and does not account for the load history of the soil.

In addressing the objective of the thesis, a numerical simulation methodology is proposed wherein the theoretical impact model is implemented. The numerical simulation methodology consists of a hydrodynamic submodel, an impact submodel and a structural submodel and is capable of accounting for site-specific parameters. The hydrodynamic and impact submodels are used in coupled time-domain simulations, whereas the structural submodel is used in un-coupled FE simulations. Impact forces obtained from time-domain simulations are compared against the structural capacity as evaluated from FE simulations to calculate structural usage factors for the simulated seastates. An assessment of an operational weather window can be made if a sufficient number of usage factors for different seastates are calculated and a safety margin is implemented into the structural evaluation criterion.

The work in this thesis shows that using site-specific weather window assessments that account for site-specific parameters, such as soil type and water depth, could definitely increase the operational weather window of SEUs and subsequently offer economic advantages to the field in which they are employed. From the case study results it is possible to conclude that the developed methodology produces smaller impact force estimates than the existing recommended practice by DNV, and that the significance of the site-specific parameter soil type is paramount on the impact forces and structural usage factors. For example, using the proposed methodology of analysis, clayey and sandy seabeds generally give impact forces that are some 75-95% and 50-80% lower, respectively, than what is simulated for a rocky seabed. Further, it has been found that the loading on the structure has two phases. The initial phase, which is studied in this thesis, is dominated by vertical forces and a following phase where horizontal forces become more significant.

9 Future work

The outcome of this thesis is a first attempt at producing a method of analysis for assessing a weather window for the installation and retrieval modes of a SEU accounting for site-specific parameters such as soil type and water depth. Several areas where additional work is required before a method can actually be established have been identified:

- It is not possible to determine the accuracy of the proposed numerical simulation methodology without making a comparison with existing methodologies. In comparison with the recommended practice by DNV (2012), see Section 2, the proposed methodology gives smaller estimates of impact forces, and, consequently, structural usage factors. This agrees well with the initial belief. However, in order to actually assess the proposed methodology and its capability to estimate impact forces and structural usage factors a comparison against measurements made on a real world, fullscale, operating SEU is necessary.
- The definition of an impact, as used in this thesis, resulted in impact forces close to vertical direction-wise. It was also noted that large horizontal forces arise on the spudcan outside this definition. It is believed that a more thorough investigation of the loading phases throughout a jacking procedure is needed to identify critical phases, recurrent phenomenon, possible amplifying effects, etc., in relation to the sensitivity of the structure. This is needed in order to extend the knowledge of the loads during impact. As an extension of this, a study aimed at clarifying the interaction between the spudcans during the jacking procedure could result in interesting and useful knowledge of loads for different incoming wave headings.
- The theoretical impact model proposed in this thesis, see Section 2.5, is capable of describing the soil-structure interaction during impact in an approximate manner. It does not account for elastic deformation of the seabed, and the effect of including elastic deformation of the soil in the impact model should be studied in order to verify the validity of the assumption of plastic deformations only. However, the main drawback of the theoretical model is its incapability of taking load history of the seabed into account, thus neglecting plasticity hardening of the soil. According to ISO (2012), bearing capacity theory is only valid for previously undisturbed soils and is thus actually only applicable to the very first contact between spudcan and seabed. In order to use it in time-domain simulations aimed at simulating the whole jacking procedure during installation or retrieval of a SEU, a theoretical model as well as a software implementation capable of handling load history is needed.
- The simulation model constructed in this thesis implements a coupled time-domain simulation containing both a hydrodynamic vessel motion model and an impact model. The advantages of coupled simulations are several, including effects on vessel motion from the impact and enabling the future possibility of simulating a full installation of a SEU. Implementing an uncoupled – simulation methodology would allow for a less software-dependent setup but effects on vessel motion from the impact would be lost. Such information is believed to be invaluable, especially if the whole jacking procedure during installation or retrieval of a SEU needs to be simulated. Therefore, it is

believed that coupled simulations are the preferred option. However, if coupled simulations should be kept as the preferred analysis method, development of the software is a must to be able to accurately simulate impact scenarios as the SIMO soil penetration tool does not have the sufficient features to correctly implement the bearing capacity theory.

- The structural capacity is evaluated quasi-statically in a separate FE model against which the impact forces are compared to obtain the structural utilization grade. However, per definition, dynamic and strain-rate effects are of great interest in impact scenarios and should be addressed. One possibility is to account for such effects by implementing a dynamic amplification factor (DAF) in the post-processing of the results from the FE simulations. Another possibility is to perform fully dynamic FE simulations based on load time-series from the time-domain. The latter approach was, however, avoided in this thesis in order to keep simulation times at a reasonable level. A third possibility could be to investigate the possibility for a fully coupled analysis, thus incorporating a simplified structural evaluation in the time-domain analysis. By doing so, dynamic effects could easily be accounted for. It does, however, require a thorough understanding of the failure modes of the structure and how to account for these in a simplified model.
- By implementing less complex analysis tools for the structural analysis, the total complexity of the method of analysis would decrease greatly. A study investigating the possibility of approximating the structural capacity of an SEU towards impact loads by, for example, an analytical beam theory is of interest. The study should also include how predefined structural limits from, for example, jacking equipment, etc., should be accounted for.
- A weather window estimate for a serviceability limit state (SLS) can be derived directly from the weather window estimate presented in Section 6.3 by introducing a safety margin. In order to do so, an investigation of what safety margin to be used is needed.
- In this thesis it has been assumed that structural capacity, incorporating yielding and buckling, is the limiting condition for the scenario under investigation. However, the structural capacity is most probably not the only factor sensitive to impact loads during the jacking procedure. The ship has a big deck with sea-fastened equipment and cargo that could be sensitive to accelerations in the impact scenario. Another important aspect to consider is crew safety. These are just two examples of factors that could be critical and an overall assessment of other parameters than structural ones should be conducted. Nonetheless, structural parameters are important and it has been noted during the work that assessments of fatigue and fracture could be necessary, especially for the failure mode in the spudcan where welds are abundant and residual stresses could greatly affect the life of the structure. The structural evaluation criterion should therefore be widened from including only the structural capacity to incorporate a full integrity check of the structure for those failure modes where it is deemed necessary.

10 References

- AeroHydro Inc. (2011): *AeroHydro MultiSurf 8.0 Version 8.0*, AeroHydro Inc., Southwest harbor, MA, USA.
- Autodesk Inc. (2013): *Autodesk Autocad 2014*, Autodesk Inc, San Rafael, CA, USA
- Bishop, R. F., Hill, R., Mott, N. F. (1945): The theory of indentation and hardness tests. *Proceedings of Physics Society*, 57, 147-159.
- Chakrabarti, P (2012): Going on location study for a jack-up rig. *Proceedings of the ASME 2012 31st International conference on Ocean, Offshore and Arctic Engineering*. July 1-6, 2012, Rio de Janeiro, Brazil.
- Danziger, F. A. B., Lunne, T. (2012): Rate Effects of Cone Penetration in Sand. *Geotechnical Engineering Journal of the SEAGS and AGSSEA* Vol. 43 No. 4 December 2012.
- Dassault Systèmes (2013): *Abaqus 6.13 Documentation*, Dassault Systèmes, Providence, RI, USA.
- DNV [Det Norske Veritas] (2013): *Wind Turbine Installation Units DNV-OS-J301*, Det Norske Veritas, Høvik, Norway.
- DNV [Det Norske Veritas] (2012): *Self-elevating Units DNV-RP-C104*, Det Norske Veritas, Høvik, Norway.
- DNV [Det Norske Veritas] (2011): *Modelling and Analysis of Marine Operations DNV-RP-H103*, Det Norske Veritas, Høvik, Norway.
- DNV [Det Norske Veritas] (2004): *Buckling strength analysis of bars and frames, and spherical shells*, Classification notes No. 30.1, Det Norske Veritas, Høvik, Norway
- Drydocks world (2010): *NG-9000C-HPE - Multi-purpose Self-propelled Jack-up*, Drydocks world – southeast Asia Pte. Limited, Singapore.
- EC [European Commission] (2008): *Offshore Wind Energy: Action needed to deliver on the Energy Policy Objectives for 2020 and beyond*, Communication From The Commission To The European Parliament, The Council, The European Economic And Social Committee And The Committee Of The Regions, Brussels, Belgium.
- Fred. Olsen Windcarrier AS (2014): *Internal document: Loading condition summary*, For inquiries, please contact the authors.
- Goldsmith, W. (1960). *Impact*, Arnold, London.
- Houlsby, G.T., Hitchman, R. (1988): Calibration chamber test of a cone penetrometer in sand. *Géotechnique* 38, No 1, 1988, pp. 39-44.
- ISO [International Organization for Standardization] (2012): *Petroleum and natural gas industries- Site-specific assessment of mobile offshore units, Part 1: Jack-ups*, ISO, ISO/DIS 19905-1, Geneva, Switzerland.
- KTH [Kungliga Tekniska Högskolan] (2007): *Handbok och formelsamling i Hållfasthetslära*, KTH, Stockholm, Sweden.
- MARINTEK [Norwegian Marine Technology Research Institute] (2013a): *SIMO – User’s manual version 4.0*, MARINTEK, Trondheim, Norway.

- MARINTEK [Norwegian Marine Technology Research Institute] (2013b): *SIMO – Theory manual version 4.0*, MARINTEK, Trondheim, Norway.
- MathWorks Inc. (2012): *MATLAB Version (R2012b)*, The MathWorks Inc., Natick, MA, USA.
- Mitchell, J. K., Brandon, T. L. (1998): Analysis and use of CPT in earthquake and environmental engineering. *Geotechnical Site Characterization, Robertson and Mayne(eds), Rotterdam, The Netherlands.*
- Poulos, Steve J. (1971): The stress-strain curves of soils. *Geotechnical engineers, Inc., Massachusetts, USA.*
- Prognos AG and Fichtner group (2013): *Cost Reduction Potential of Offshore Wind Power in Germany*. Berlin, 2013.
- R.E.H. Sims, R.N. Schock, A. Adegbululgbé, J. Fenhann, I. Konstantinaviciute, W. Moomaw, H.B. Nimir, B. Schlamadinger, J. Torres-Martínez, C. Turner, Y. Uchiyama, S.J.V. Vuori, N. Wamukonya, X. Zhang (2007): *Energy supply*. In *Climate Change 2007: Mitigation*. Contribution of Working Group III to the Fourth Assessment Report of the Intergovernmental Panel on Climate Change [B. Metz, O.R. Davidson, P.R. Bosch, R. Dave, L.A. Meyer (eds)], Cambridge University Press, Cambridge, United Kingdom and New York, NY, USA.
- Statoil ASA (2006): *Extract from internal document*. For inquiries, please contact Rune Yttervik.
- Sällfors, G., (2009): *Geoteknik*. Chalmers University of Technology, Gothenburg, Sweden
- The Society of Naval Architects and Marine Engineers [SNAME] (2008): *Recommended Practice for Site Specific Assessment of Jack-Up Units*. The Society of Naval Architects and Marine Engineers. Houston, Texas.
- Verruijt, A., (2012): *Soil mechanics*. Delft University of Technology, Delft, The Netherlands.
- Walker J., Yu, H. S. (2006): Adaptive finite elements analysis of cone penetration in clay, *Acta Geotechnica*, No 1, April 2006, pp. 43-57
- WAMIT Inc (2013): *WAMIT User manual Version 7.0*, WAMIT Inc., Chestnut Hill, MA, USA.
- Williams, M. S., Thompson, R.S.G., Houlsby, G.T. (1997): *Non-linear dynamic analysis of offshore jack-up unit*, University of Oxford, Department of Engineering Science, Oxford, United Kingdom.

Appendix A Hydrodynamic model

This appendix contains a detailed description of the hydrodynamic model used for time-domain simulations in SIMA/SIMO. The terminology used here is explained in MARINTEK (2013) and WAMIT Inc. (2013).

Several coordinate systems are used, see Figure A.1. No 1 is the local coordinate system for the hull, which in the initial condition coincides with the global coordinate system. No 2 is the local coordinate system used for modelling of the slender elements, representing the legs, and No 3 is the local coordinate system for the separate body representing a spudcan. The colours represent the coordinate axis, red translates to x-axis, blue to y-axis and green to z-axis.

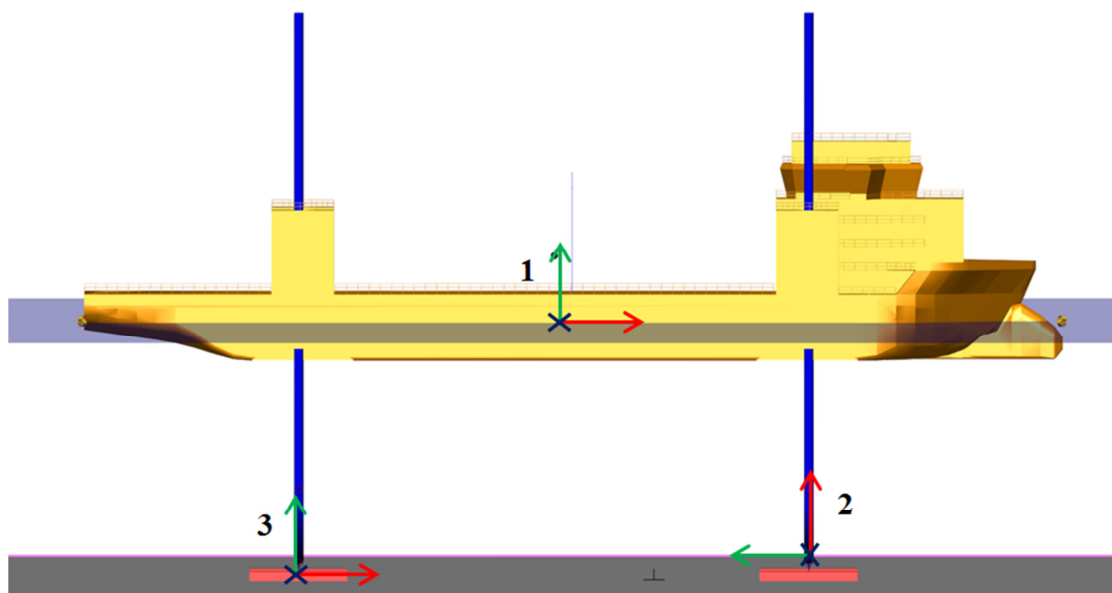


Figure A.1 Coordinate systems used in the time-domain simulations in SIMA/SIMO. An external geometry file is used for the vessel geometry, courtesy of Fred. Olsen Windcarrier AS.

A.1 Hull model

The hull is modelled as a "large body" in SIMA/SIMO, thus allowing for motions in all 6 DOFs. Table A.1 shows the structural mass model specified by the user for the vessel. Table A.2 and A.3 shows hydrostatic stiffness and added mass as being an output from WAMIT, which is used in time-domain simulations to calculate the motions of the vessel in waves. Figure A.2 shows some important first-order motion transfer function (RAOs) for the vessel.

Table A.1 Structural mass model of vessel.

Mass [kg]	I_{xx} [kgm ²]	I_{yy} [kgm ²]	I_{zz} [kgm ²]
1.806×10^7	1.463×10^9	1.625×10^{10}	1.625×10^{10}

Table A.2 Hydrostatic stiffness in 6 DOF. Purely translational elements are given in [N/m], purely rotational elements in [Nm] and combinations in [N].

	Surge	Sway	Heave	Roll	Pitch	Yaw
Surge	0	0	0	0	0	0
Sway	0	0	0	0	0	0
Heave	0	0	4.467×10^7	0	3.405×10^8	0
Roll	0	0	0	2.822×10^9	0	0
Pitch	0	0	3.405×10^8	0	5.075×10^{10}	0
Yaw	0	0	0	0	0	0

Table A.3 Added mass in 6 DOF. Purely translational elements are given in [kg], purely rotational elements in [kgm²] and combinations in [kgm].

	Surge	Sway	Heave	Roll	Pitch	Yaw
Surge	5.386×10^6	0	1.552×10^6	0	9.630×10^7	0
Sway	0	2.205×10^6	0	-1.257×10^7	0	1.081×10^7
Heave	1.552×10^6	0	6.947×10^7	0	4.459×10^8	0
Roll	0	-1.259×10^7	0	3.367×10^9	0	1.223×10^7
Pitch	9.647×10^7	0	4.458×10^8	0	5.894×10^{10}	0
Yaw	0	1.076×10^7	0	1.176×10^7	0	2.299×10^9

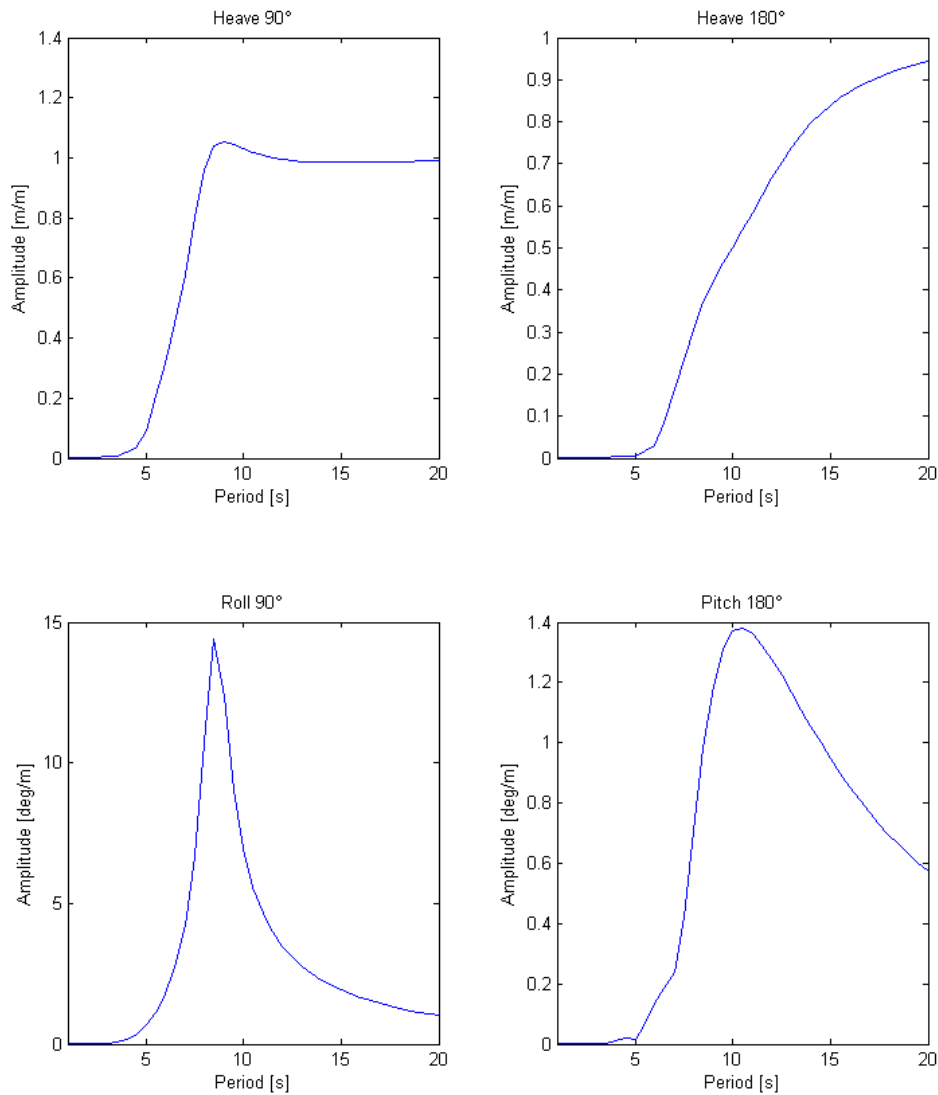


Figure A.2 A selection of First Order Motion Transfer functions (RAOs) for the hull model.

A.2 Leg model

The legs are modelled as slender elements with specific volume, 1.173 m^2 and distributed mass, $8.780 \times 10^3 \text{ kg/m}$. The mass of the legs are thus added to the mass matrix given for the hull model in the time-domain simulations. Quadratic drag and added mass coefficients in the transverse direction are also included in the model as specified below.

Quadratic drag coefficients, for use in the Morrison equation, for drag forces acting transversely on the legs are calculated for a unit length as:

$$\frac{F_D}{u_a^2} = \frac{1}{2} \rho C_D D \quad (\text{A.1})$$

where:

C_D is the dimensionless drag coefficient, taken as 1.0 in this case.

D is the diameter of the cylinder.

It is assumed that the legs may be approximated as solid cylinders. Drag coefficients are identical in the tangential and transverse directions, $2.306 \times 10^3 \text{ N s}^2/\text{m}^3$.

Added mass of the cylinder is calculated per unit length using:

$$m_a = \rho \pi R^2 \quad (\text{A.2})$$

where:

ρ is the density of the fluid surrounding the cylinder.

R is the radius of the cylinder.

The assumption of a solid cylinder with radius as the outer radius of a leg is made. Added mass in y- and z-direction (transverse directions) are identical, 16302 kg/m.

A.3 Spudcan model

The spudcans are modelled as small bodies, thus only allowing for motions in 3 DOF. No rotations are accounted for. A small body is considered as a point mass, thus no moments of inertia are given for the spudcan. The structural mass of one spudcan amounts to $2.978 \times 10^5 \text{ kg}$.

Quadratic drag and added mass coefficients are included in the model as presented in Table A.4. Quadratic drag coefficients are estimated using table A.1 in DNV (2011). Added mass is estimated using table A.2 in DNV (2011).

Table A.4 Quadratic drag and added mass for one spudcan.

	<i>x-dir</i>	<i>y-dir</i>	<i>z-dir</i>
<i>Quadratic drag [Ns²/m³]</i>	1.376×10^4	1.738×10^4	6.265×10^4
<i>Added mass [kg]</i>	3.135×10^4	5.230×10^4	4.908×10^5

A.4 Coupling model

Fixed elongation couplings are used to couple legs and spudcans. Stiffness and damping properties of the couplings are chosen so as to represent the stiffness and damping of a leg and are obtained from the FE model of the leg and spudcan as presented in the report. Stiffness proportional damping is used, 1% in the axial direction and 5% in the transverse direction. Axial and transverse stiffness and damping used for representing the flexibility of the leg is presented in Table A.5.

Table A.5 Stiffness and damping representing the leg

	<i>Axial</i>	<i>Transverse</i>
<i>Stiffness [N/m]</i>	4.4×10^9	4.0×10^7
<i>Damping [Ns/m]</i>	4.4×10^7	2.0×10^6

A.5 Horizontal anchor system

Fixed force elongations, using the “pretension and local direction” method, are used for station keeping of the vessel during the course of a simulation. Four couplings are used in the directions 45 degrees, 135 degrees, 225 degrees and 315 degrees with stiffness parameter 7.070×10^5 N/m and pretension 5×10^5 N.

Appendix B Geotechnical model

The soil interaction on the analysed structure has been made using the soil interaction tool in SIMA. The input parameters for this tool have been evaluated using a methodology recommended in ISO 19905-1-2012 and “Recommended Practice for Site Specific Assessment of Jack-Up Units” published by SNAME 2008. The methodology and the model will be described more in detail in this Appendix.

The objective of the geotechnical model is to evaluate the soil friction forces vertically and horizontally. The friction forces can also be denoted bearing capacity. The output parameters are split up into three different factors.

- Downward friction force, the bearing force against a spudcan penetrating the soil.
- Upward friction force, the “suction force” that acts on the spudcan when full penetration has been achieved and the spudcan has an upward force.
- Horizontal friction force, the friction force acting on the spudcans horizontally.

All of these forces are dependent of the penetration depth, the geometry of the penetrating body and the material parameters of the soil. The geotechnical model used in this report is built in Microsoft Excel 2010 and considers both clays and silica sands.

B.1 Silica sands

The material parameters needed in the calculation of the bearing forces in sand is the internal friction angle [degrees] and the heaviness of the material [$\frac{N}{m^3}$]. The rest of the parameters are calculated from them.

Table B.1 Parameters affecting vertical bearing, values presented for sand $\varphi=35$ degrees.

<i>Parameter</i>	<i>Value</i>	<i>Unit</i>	<i>Description</i>
φ	35	[deg]	Friction angle of the sand
N_γ	41.9	[-]	Bearing factor
N_q	80.8	[-]	Bearing factor
γ'	9000	[N/m ³]	Submerged unit weight of the soils
d_γ	1	[-]	Depth factor on surcharge for drained soils
p'	0	[-]	If the spud can penetrates beyond its widest point, the overburden of soil above this point creates an effective surcharge, p'_0 , at the level of its widest point, which leads to additional bearing capacity,(=0, assuming no backfill)

Table B.2 Parameters affecting horizontal bearing, values presented for sand $\varphi=35$ degrees.

Parameter	Value	Unit	Description
h_1	[-]	[m]	Embedment depth (h_1+h_2 =Penetration depth).
h_2	[-]	[m]	Spudcan tip embedment depth (h_1+h_2 =Penetration depth).
k_a	0.27	[-]	Active earth pressure coefficient
k_p	3.69	[-]	Passive earth pressure coefficient
δ	30	[deg]	Steel/soil friction angle in degrees (taken as $(\varphi - 5)$, for a flat plate)

Table B.3 Resulting bearing forces for sand $\varphi=35$ degrees.

Depth [m]	Down [MN]	Up [N]	Horizontal [MN]
0.00	0.128	0.0	0.0
-0.07	0.136	0.0	0.079
-0.14	0.145	0.0	0.084
-0.21	0.154	0.0	0.090
-0.28	0.162	0.0	0.097
-0.35	0.172	0.0	0.105
-0.42	0.181	0.0	0.114
-0.49	0.190	0.0	0.125
-0.56	0.200	0.0	0.139
-0.63	0.210	0.0	0.155
-0.70	0.220	0.0	0.172
-0.77	0.230	0.0	0.193
-0.84	0.240	0.0	0.217
-0.91	0.250	0.0	0.245
-0.98	1.764	0.0	1.160
-1.05	9.021	0.0	5.427
-1.12	19.347	0.0	11.501
-1.19	32.004	0.0	18.960
-1.26	46.622	0.0	27.594
-1.33	62.965	0.0	37.272
-1.40	80.868	0.0	47.903
-1.47	100.205	0.0	59.420
-1.54	234.368	0.0	137.379
-1.61	234.368	0.0	137.938
-1.68	234.368	0.0	138.558

B.2 Clays

The material parameters needed in the calculation of the bearing forces in clays is the shear strength and the heaviness of the material $[\frac{N}{m^3}]$. The rest of the parameters are calculated from them.

Table B.4 Parameters affecting vertical bearing capacity, values presented for clay $s_u = 100 \text{ kPa}$.

<i>Parameter</i>	<i>Value</i>	<i>Unit</i>	<i>Description</i>
s_u	100000	[Pa]	Shear strength of the clay
N_c	6.0	[-]	Shape and depth factors ($N_c * s_c = 6$)
s_c			
p'_0	0	[-]	Effective overburden pressure at depth, D , of maximum bearing. (Assuming no backfill)

Table B.5 Parameters affecting horizontal bearing capacity, values presented for clay $s_u = 100 \text{ kPa}$.

<i>Parameter</i>	<i>Value</i>	<i>Unit</i>	<i>Description</i>
s_u	100000	[Pa]	Shear strength of clay.
s_{ua}	100000	[Pa]	Undrained shear strength of backfill material above the spudcan (Assumed s_u).
s_{ul}	100000	[Pa]	Undisturbed undrained shear strength at the spud can tip (Assumed s_u , homogenous material).
s_{u0}	100000	[Pa]	Undisturbed undrained shear strength at deepest depth of maximum bearing area (Assumed s_u , homogenous material).

Table B.6 Resulting bearing forces for clay $s_u = 100\text{kPa}$.

Depth [m]	Down [MN]	Up [MN]	Horizontal [MN]
0.0	0.0	0.0	0.0
-0.1	0.452	-0.271	0.106
-0.1	0.477	-0.286	0.125
-0.2	0.503	-0.301	0.147
-0.3	0.528	-0.317	0.171
-0.4	0.555	-0.332	0.196
-0.4	0.581	-0.348	0.223
-0.5	0.607	-0.364	0.251
-0.6	0.634	-0.380	0.282
-0.6	0.661	-0.396	0.314
-0.7	0.688	-0.413	0.348
-0.8	0.716	-0.429	0.383
-0.8	0.743	-0.446	0.420
-0.9	0.771	-0.463	0.458
-1.0	1.950	-1.170	0.775
-1.1	5.012	-3.007	1.296
-1.1	8.052	-4.831	1.727
-1.2	11.087	-6.652	2.135
-1.3	14.120	-8.472	2.536
-1.3	17.153	-10.292	2.938
-1.4	20.187	-12.112	3.343
-1.5	23.222	-13.933	3.755
-1.5	65.689	-39.413	6.520
-1.6	65.766	-39.459	6.821
-1.7	65.843	-39.506	7.122

Appendix C FE simulation results

The failure surfaces used in this report are built up by a number of FE simulations that are conducted to evaluate the structural capacity of the leg and spudcan. The simulations were made for three different vertical planes and the number of simulations were adjusted so that the piecewise linear curve is representative of the structural capacity.

C.1 Failure modes

The failure curves presented in Section 6.2 represent the critical failure mode for each load direction in the evaluation. Two different modes are identified in that evaluation. However, two other modes have been identified as critical for the structural evaluation criteria. For example, yielding in the top plate of the spudcan is critical for the vertical load case, but there are buckling modes that occur at greater magnitudes. The first buckling mode for the vertical will be presented followed by the first critical failure mode for yielding.

The critical buckling mode for the vertical load case is governed by the compressive stresses in the top plate where the leg is attached to the spudcan. The load governs local buckling in one of the top stiffeners as shown in Figure C.1. The load corresponding to the response can be described by the load vector:

$$\mathbf{F}_{cr} = \begin{bmatrix} 0 \\ 0 \\ 302 \end{bmatrix} MN.$$

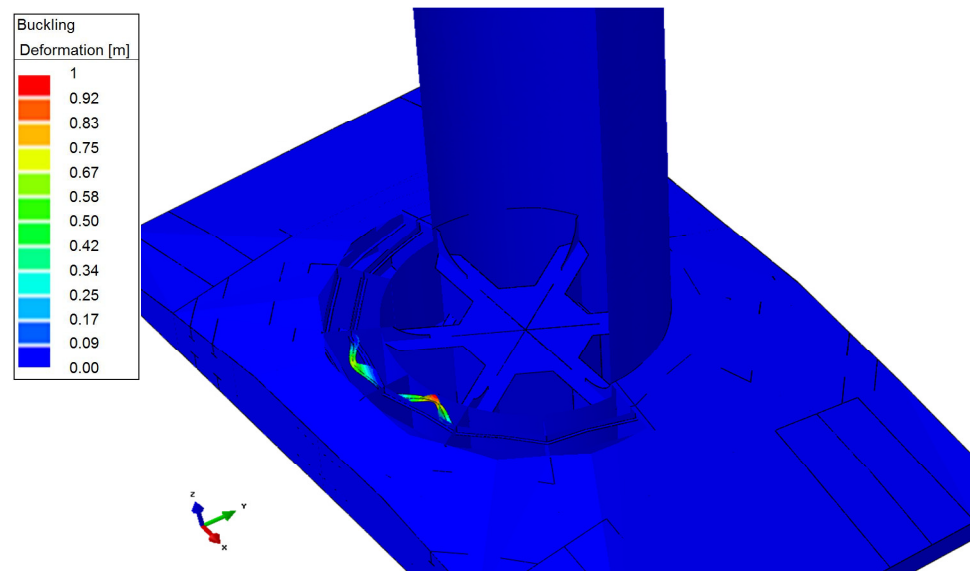


Figure C.1 The top T-profile stiffeners are the critical region with regard to buckling for vertical loads acting on the bottom plate.

The critical failure mode when it comes to yielding in the horizontal load cases are strongly connected to the buckling mode as it occurs in the top holes of the leg. The failure mode is presented in Figure C.2 and the corresponding load can be described

by: $\mathbf{F}_{cr} = \begin{bmatrix} 8.8 \\ 0 \\ 0 \end{bmatrix} MN.$

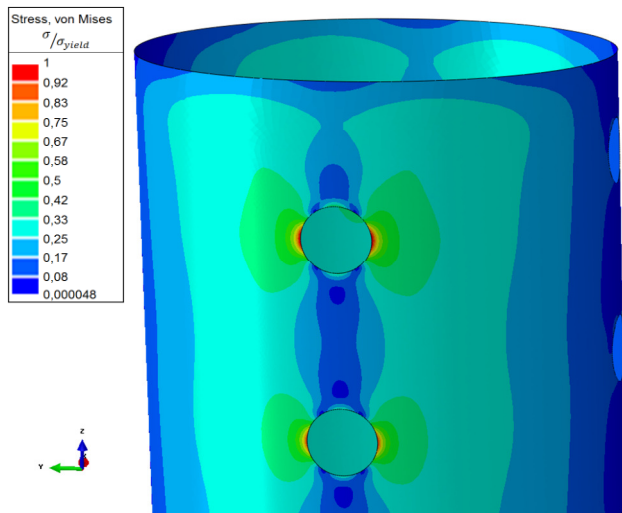


Figure C.2 The top holes of the leg are the critical region with regard to yielding for horizontal loads acting on the bottom plate in head seas (x -dir).

C.2 FE results

The structural capacity is presented in tables below followed by descriptions of the identified failure modes. The component directions are shown in Figure C.3.



Figure C.3 The analyzed structure in its coordinate system.

Table C.1 FE simulation results to describe the failure surface in the X-Z plane.

Load direction	Yield failure		Elastic buckling failure	
	Magnitude	Critical area	Magnitude (MN)	Critical mode
[1 0 0]	8.80	Top holes	141	Top hole
[1 0 1]	11.88	Top holes	193	Top hole
[1 0 2]	18.34	Top holes	295	Top hole
[1 0 4]	32.98	Top holes	510	Top hole
[1 0 6]	45.62	Top holes	709	Top hole
[1 0 10]	70.33	Top holes	1076	Top hole
[1 0 15]	100.22	Top holes	1140	Spudcan
[1 0 20]	120.15	Spudcan	1146	Spudcan
[0 0 1]	130.00	Spudcan	1153	Spudcan

Table C.2 FE simulation results to describe the failure surface in the Y-Z plane.

Load direction	Yield failure		Elastic buckling failure	
	Magnitude	Critical area	Magnitude (MN)	Critical mode
[0 1 0]	8.80	Top holes	141	Top hole
[0 1 1]	12.16	Top holes	193	Top hole
[0 1 2]	18.34	Top holes	295	Top hole
[0 1 4]	32.98	Top holes	510	Top hole
[0 1 6]	45.62	Top holes	709	Top hole
[0 1 10]	70.33	Top holes	1076	Top hole
[0 1 15]	100.22	Top holes	1140	Spudcan
[0 1 20]	120.15	Spudcan	1146	Spudcan
[0 0 1]	130.00	Spudcan	1153	Spudcan

Table C.3 FE simulation results to describe the failure surface in the XY-Z plane.

Load direction	Yielding failure		Elastic buckling failure	
	Magnitude	Critical area	Magnitude (MN)	Critical mode
$[\frac{1}{\sqrt{2}} \frac{1}{\sqrt{2}} 0]$	8.10	Top holes	161	Top hole
$[\frac{1}{\sqrt{2}} \frac{1}{\sqrt{2}} 1]$	11.24	Top holes	192	Top hole
$[\frac{1}{\sqrt{2}} \frac{1}{\sqrt{2}} 2]$	17.44	Top holes	264	Top hole
$[\frac{1}{\sqrt{2}} \frac{1}{\sqrt{2}} 4]$	30.51	Top holes	434	Top hole
$[\frac{1}{\sqrt{2}} \frac{1}{\sqrt{2}} 6]$	42.58	Top holes	600	Top hole
$[\frac{1}{\sqrt{2}} \frac{1}{\sqrt{2}} 10]$	62.31	Top holes	896	Top hole
$[\frac{1}{\sqrt{2}} \frac{1}{\sqrt{2}} 15]$	90.20	Top holes	1127	Spudcan
$[\frac{1}{\sqrt{2}} \frac{1}{\sqrt{2}} 20]$	116.14	Spudcan	1138	Spudcan
$[0 0 1]$	0	Spudcan	1153	Spudcan